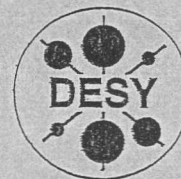


2
DEUTSCHES ELEKTRONEN-SYNCHROTRON



DESY-THESIS-1998-032
September 1998



X1998-01605

Screening Masses in the Symmetric Phase
of the Standard Model

by

F. Eberlein



ISSN 1435-8085

NOTKESTRASSE 85 - 22607 HAMBURG

DESY behält sich alle Rechte für den Fall der Schutzrechtserteilung und für die wirtschaftliche Verwertung der in diesem Bericht enthaltenen Informationen vor.

DESY reserves all rights for commercial use of information included in this report, especially in case of filing application for or grant of patents.

To be sure that your reports and preprints are promptly included in the HEP literature database send them to (if possible by air mail):

DESY
Zentralbibliothek
Notkestraße 85
22603 Hamburg
Germany

DESY
Bibliothek
Platanenallee 6
15738 Zeuthen
Germany

Screening Masses in the Symmetric Phase of the Standard Model

Dissertation
zur Erlangung des Doktorgrades
des Fachbereichs Physik
der Universität Hamburg

vorgelegt von
Frank Eberlein ✓
aus Gunzenhausen

Hamburg
1998

Gutachter der Dissertation: Prof. Dr. W. Buchmüller
Prof. Dr. G. Mack

Gutachter der Disputation: Prof. Dr. W. Buchmüller
Prof. Dr. J. Bartels

Datum der Disputation: 11. Sept. 1998

Dekan des Fachbereichs Physik
und Vorsitzender des
Promotionsausschusses:

Prof. Dr. B. Kramer

Abstract

The screening masses in a 3-dimensional gauge theory can be calculated analytically using gap equations. This mechanism is extended to two-loop order. We calculate the two-loop gap equation in a resummed non-linear σ -model and in a resummed $SU(2)$ Higgs model. The corresponding self-energies of the vector boson and the Higgs field are evaluated in Feynman and in unitary gauge. We demonstrate that in both theories the two-loop gap mass is in good agreement with the one-loop results and with lattice data. In the non-linear σ -model, the two-loop propagator mass is $\approx 0.34 g^2$ and numerically nearly independent of the gauge parameter. In the Higgs model, the two-loop gap equation is solved in Feynman gauge yielding $m \approx 0.31 g^2$.

Zusammenfassung

Die Abschirmmassen einer dreidimensionalen Eichtheorie kann man mit Hilfe von Gapgleichungen analytisch berechnen. Dieser Mechanismus wird auf Zwei-Schleifen-Ordnung erweitert. Wir stellen die Zwei-Schleifen-Gapgleichung in einem resummierten nicht-linearen σ -Modell und in einem resummierten $SU(2)$ -Higgsmodell auf. Die entsprechenden Selbstenergien des Vektorbosons und des Higgsfeldes werden in Feynman- und in unitärer Eichung berechnet. Wir zeigen, daß die Zwei-Schleifen-Gapmasse in beiden Theorien in guter Übereinstimmung mit den Ein-Schleifen-Ergebnissen und den Gitterdaten ist. Im nicht-linearen σ -Modell ist die Propagatormasse in Zwei-Schleifen-Ordnung $\approx 0.34 g^2$ und numerisch nahezu unabhängig vom Eichparameter. Im Higgsmodell wird die Gapgleichung auf Zwei-Schleifen-Niveau in Feynman-Eichung gelöst und es ergibt sich $m \approx 0.31 g^2$.

Contents

Introduction	1
1 The Problem of the Magnetic Mass	4
1.1 Infrared divergences and resummation	4
1.2 The 3-dimensional reduced theory and its renormalization properties	6
1.3 Lattice simulations in the symmetric phase	8
2 One-loop Gap Equations	11
2.1 Gap equation principles	11
2.2 The $SU(2)$ Higgs model	13
2.3 The non-linear σ -model	17
2.4 Peculiarities of the unitary gauge	19
2.5 Other one-loop calculations	20
3 Calculation Techniques for Two-loop Propagator Integrals	22
3.1 The concept of reducing scalar integrals to basic integrals	22
3.2 Recurrence relations	24
4 Two-loop Gap Equation in the Non-linear σ -model	28
4.1 Further simplifications of the model	28
4.2 Motivations for a two-loop calculation	30
4.3 Two-loop self-energy in resummed massive Yang-Mills theory	30
4.4 Two-loop calculation in renormalizable gauges	34
4.5 Two-loop gap equation in the non-linear σ -model	37

5 Two-loop Gap Equation in the $SU(2)$ Higgs Model	39
5.1 One-loop gap equations revisited: Landau versus Feynman gauge	39
5.2 Two-loop self-energy for the Higgs field	41
5.3 Two-loop self-energy for the vector field	41
5.4 Two-loop gap equation for the vector boson	47
Summary and Conclusions	53
A One-loop Integrals	55
B Two-loop Results in the Non-linear σ -model	57
C Basic Integrals in $d = 3 - 2\epsilon$	60
D Two-loop Results in the $SU(2)$ Higgs Model	64
E Numerical Evaluation of the Master Integral	71

Introduction

One of the most interesting unsolved problems in elementary particle physics and cosmology is the baryon asymmetry in the observed universe [1]. Quantitatively, it is

$$Y_B = \frac{n_B - n_{\bar{B}}}{s} \approx 10^{-10}, \quad (0.1)$$

with $n_{B,\bar{B}}$ being the baryon and antibaryon density, respectively, and s being the entropy density in a comoving volume. As an example, the lack of a considerable amount of antimatter in our galaxy cluster cannot be explained by any known mechanism to separate matter and antimatter on this length scale.

In principle, the baryon asymmetry can be introduced into the cosmological Standard Model as an initial condition. In the evolution of the universe there are, however, baryon number violating processes which may wash out the initial asymmetry. To treat the baryon asymmetry as an initial condition is also not compatible with inflationary models [1]. For these reasons, it is expected to be generated dynamically during the evolution of the universe.

Sakharov pointed out three basic requirements, which have to be fulfilled for dynamical baryogenesis [2]. These are *i*) baryon number violating processes, *ii*) C- and CP-violation and *iii*) departure from thermal equilibrium.

The last possible stage in the evolution of the early universe for the generation of the observed baryon asymmetry, is the electroweak phase transition, which occurred 10^{-10} seconds after the big bang [3]. Baryon-number violating processes fall out of thermal equilibrium at the corresponding critical temperature. The electroweak phase transition is the transition from a high-temperature, symmetric phase to a broken phase with the familiar massive W - and Z -Bosons and massless photons. It is connected with a jump of the Higgs vacuum expectation value, which is small in the symmetric phase, to a much higher value in the broken phase. The phase transition in the corresponding finite temperature quantum field theory was first investigated in [4].

It is now known that the electroweak phase transition is only of first order for Higgs masses

below 70 GeV [5]. Around 80 GeV it changes to a smooth crossover. In this case, there is no departure from thermal equilibrium at the phase transition and the Standard Model baryogenesis seems to be ruled out.

Hence, the baryon asymmetry has to be generated at energies higher than the electroweak scale. There have been many attempts to explain baryogenesis in the framework of Grand unified theories (GUT's), where baryon number violating processes are already possible at tree-level [1]. However, this scenario may lead to problems with inflation, which demands reheating temperatures well below the GUT scale [6]. Taking this into account, baryogenesis between the reheating scale and the electroweak scale has recently been investigated in [7] using the gauge group $SO(10)$. It has been shown that the observed baryon asymmetry can be generated in non-supersymmetric as well as in supersymmetric theories.

Any generated baryon asymmetry will partly be washed out in the symmetric phase of the Standard model, as baryon number violating processes are expected to occur rapidly at high temperatures. The exact value of the rate at which these processes occur, the sphaleron-rate, is not yet known in the high-temperature phase. In recent years, there has been intensive research to estimate this rate [8].

In the high-temperature phase of the Standard Model, there are still technical and conceptual problems. One naively expects a vanishing Higgs vacuum expectation value and vector boson mass. This leads to a breakdown of the perturbative expansion due to severe infrared divergences in the magnetic sector of the theory [9]. This infrared problem may be cured by introducing a non-vanishing magnetic mass, which acts as a cutoff regularizing these divergences. The symmetric phase is expected to be governed by non-perturbative effects whose size is determined by the magnetic screening length, which is the inverse of this magnetic mass.

The picture of the symmetric phase which one has obtained so far, mainly on the lattice [20], is one of a confining phase with a dense spectrum of bound states (W -balls and bound states of scalars). Other simulations [21] could extract a propagator mass for the vector boson which is much smaller than the mass of the lightest bound state. The correlation between the different masses, the origin of the magnetic mass, its connection with confinement and with the particle content in the symmetric phase is still not known.

At high temperatures the 4-dimensional finite temperature field theory can be described by an effective 3-dimensional theory. An analytical framework for calculating the dynamically generated mass in a 3-dimensional $SU(2)$ gauge theory has recently been via gap equations, which so far have been treated only to one-loop order. The extension to two loops is the central topic of this thesis. It

is a crucial test for the reliability of the method. The two-loop results indicate that gap equations are a consistent tool to calculate the propagator mass for the vector boson in 3 dimensions.

In chapter 1, we draw the physical picture of the symmetric phase which was obtained so far, mainly in lattice calculations. We describe the main open questions and the connection between the 3-dimensional Higgs model and the high-temperature expansion of the corresponding finite temperature quantum field theory in 4 dimensions.

In chapter 2, the concept of gap equations is presented, which has recently been used by several authors to calculate the magnetic mass. The one-loop results in the 3-dimensional non-linear σ -model and the Higgs model are reviewed and the vector boson and Higgs self-energies are newly calculated to this order in unitary gauge. Furthermore, the peculiarities of calculations in unitary gauge are thoroughly discussed and the problems with renormalization are described. It is shown that the solution of the gap equation in the non-linear σ -model provides a very good approximation to the gap mass in the Higgs model to one-loop order.

Chapter 3 deals with technical aspects of the two-loop calculation. We explain in detail a recently developed algorithm [37], which is used to reduce two-loop Feynman integrals to a set of linearly independent basic integrals.

In Chapter 4, the two-loop calculation in the non-linear σ -model is presented keeping the gauge parameter arbitrary. It is seen that the two-loop gap equation has a real and positive solution. The two-loop correction to the one-loop gap mass turns out to be small and numerically nearly independent of the gauge-fixing parameter and the renormalization scale.

To test the non-linear σ -model as a model for infrared phenomena in the symmetric phase, an analogous calculation is performed in chapter 5 for the 3-dimensional $SU(2)$ Higgs model. The self-energy of the Higgs field and the transverse part of the polarization tensor of the vector boson is calculated in unitary and Feynman gauge. The analysis of the two-loop gap equation for the vector boson mass in Feynman gauge shows that the two-loop correction to the gap mass in the linear model is of the same sign and of similar size as in the non-linear σ -model.

In appendix A, we summarize the formulae for one-loop integrals in 3 dimensions in dimensional as well as cut-off regularization. In appendix B, the two-loop results of the non-linear σ -model are presented in more detail keeping the dimension arbitrary. Appendix C summarizes the basic two-loop integrals. In appendix D, the two-loop Higgs and vector boson self-energy in the $SU(2)$ Higgs model are given in unitary and Feynman gauge, and finally in appendix E the two-loop master integral is evaluated numerically for several special mass cases.

Chapter 1

The Problem of the Magnetic Mass

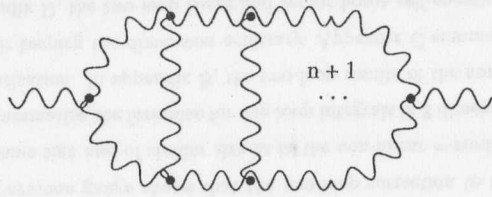
In this introductory chapter, we sketch the basic unsolved problems in the high-temperature phase of the Standard model. We also describe the relation between a 4-dimensional finite temperature field theory and the corresponding 3-dimensional $T=0$ theory, which justifies the restriction to 3-dimensional gauge-Higgs models in the two-loop calculation. At the end of this chapter, we present the main features of the physical picture of the symmetric phase which one has obtained so far, mainly in lattice simulations.

1.1. Infrared divergences and resummation

An extensive overview of finite temperature quantum field theory can nowadays already be found in textbooks [11]. The main difference to $T=0$ field theory is that in the partition function, which is the equivalent of the generating functional, one integrates over a finite interval $[0, \beta]$ in imaginary time. Fourier-transformation leads to discrete Matsubara-frequencies $\omega_n = 2n\pi T$ for bosons and $\omega_n = (2n + 1)\pi T$ for fermions.

It turns out, that the behaviour in the UV is exactly the same as in $T=0$ field theory. The renormalization counter-terms for $T=0$ are sufficient to render all thermodynamic quantities in the corresponding finite temperature field theory finite. However, there are complications in the infrared. Compared to $T=0$ quantum field theory, one encounters additional severe infrared divergences, as can already be seen in the following simple example.

Consider the static infrared limit of the vector boson self energy in a non-Abelian $SU(N)$ -gauge theory (the static modes yield the dominant infrared contribution). The contribution of a typical

Figure 1.1: $(n+1)$ -loop diagram contributing to the vector boson self-energy

$(n+1)$ -loop diagram in fig. 1.1 can be estimated as follows,

$$g^{2n+2} \left(T \int d^3p \right)^{n+1} p^{2n+2} (p^2 + m^2)^{-(3n+2)}, \quad (1.1)$$

where the external momentum has been set to zero for simplicity. After integration this is of the order

$$g^4 T^2 \left(\frac{g^2 T}{m} \right)^{n-1}, \quad n > 1, \quad (1.2)$$

If the internal particles are massless, the contribution to the self-energy is divergent. However, the originally massless gauge bosons get a dynamically generated mass which is temperature dependent. The self-energy for static fields behaves for small external momentum as [13]

$$\Pi_{\mu\nu}(p_0 = 0, p \rightarrow 0) = \delta_{\mu 0} \delta_{\nu 0} \frac{N}{3} g^2 T^2 + O(p), \quad (1.3)$$

where one can extract an electric mass

$$m_{el}^2 = \Pi_{00}(p_0 = 0, p \rightarrow 0) = \frac{N}{3} g^2 T^2 \quad (1.4)$$

for the A_0 fields. The spatial components A_i remain massless to this order.

The crucial point is, that the electric mass is of the order of the coupling. Therefore, for soft momenta $p \sim gT$, the one-loop self-energy is of the same order as the inverse of the tree-level transverse propagator $p^2 g_{\mu\nu} - p_\mu p_\nu \sim g^2 T^2$. In order to calculate consistently in perturbation theory, the tree-level propagator has to be modified to incorporate contributions of higher-order loop diagrams which are already relevant to leading order in g . The simple connection between loop order and the order in the coupling constant of $T=0$ field theories is no longer valid at finite temperature. In [12], Braaten and Pisarski established a program for a systematic resummation of the perturbation series, which allows a complete calculation of amplitudes to a given order in g (as long as infrared divergences are screened by a mass $\sim gT$). If the external fields are static, there

is a considerable simplification of the resummation program [14], the well-known ring summation of daisy and super-daisy graphs. The summation of all the ring-diagrams is equivalent to replacing the tree-level propagator by a corrected propagator which involves the one-loop mass of above [15,16]. This procedure removes the infrared infinities for all internal lines of the A_0 -field.

There remains a problem with the A_i -fields, however. As they do not get a mass to one-loop order, the magnetic mass is at least of second order in the coupling $m \sim g^2 T$. From (1.2), one immediately sees that such a mass would get contributions from all orders in perturbation theory. In other words, it is not perturbatively calculable.

The purpose of this dissertation is to shed light on the generation of this magnetic mass and, in particular, to extend and thereby check a formalism for calculating its numerical value, which is based on gap equations.

1.2 The 3-dimensional reduced theory and its renormalization properties

An extensive overview of the ideas of dimensional reduction as well as the calculations can best be found in [17]. Here, the main steps are summarized and the renormalization properties of the 3-dimensional theory are discussed.

We are interested in the high-temperature phase of the electroweak Standard Model, the focus being on the infrared content of the theory, i. e. we would like to study the theory at scales $\sim g^2 T$. Originally, there are a number of different mass scales in finite-temperature electroweak theory: the temperature T , the scale of the Debye mass or the electric mass gT , the non-perturbative magnetic mass $g^2 T$ etc. For our purpose, it is very helpful to integrate out all modes which are heavier than $g^2 T$.

As already outlined in the previous section, in finite-temperature field theory we have discrete Matsubara frequencies due to a finite integration in imaginary time. The 4-dimensional finite temperature field theory can be viewed as a 3-dimensional $T=0$ theory with an infinite number of excitations. Their masses are $m^2 + (2\pi nT)^2$ for bosons and $m^2 + (2\pi(n+1)T)^2$ for fermions. In [18] all these massive degrees of freedom, namely all fermionic modes and all bosonic modes except for $n=0$, are integrated out. This is the program of dimensional reduction of hot 4-dimensional theories at finite temperature.

More explicitly, let us consider the following 4-dimensional Lagrangian

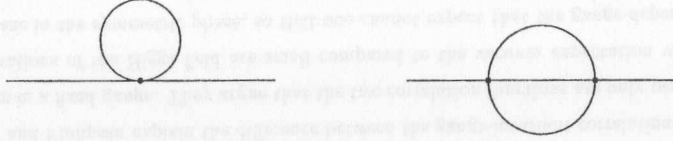


Figure 1.2: UV-divergent topologies in the 3-dimensional Higgs model

$$\mathcal{L} = \frac{1}{4} F_{\mu\nu}^a F_{\mu\nu}^a + (D_\mu \Phi)^\dagger (D_\mu \Phi) - \frac{1}{2} m^2 \Phi^\dagger \Phi + \lambda (\Phi^\dagger \Phi)^2. \quad (1.5)$$

We neglect fermions for simplicity, which lead to more complicated equations, but do not incorporate new infrared physics. They can be added to (1.5) in a straightforward way [14,19]. Instead of starting with the whole electroweak Standard Model, we therefore restrict ourselves to the $SU(2)$ gauge theory with a doublet scalar field.

Integrating out all modes $\sim T$ leads to the following effective action for energies $\sim gT$

$$S_{\text{eff}}[A_i^a(x), A_0^a(x), \Phi_i(x)] = \int d^3x \left\{ \frac{1}{4} F_{ij}^a F_{ij}^a + \frac{1}{2} (D_i A_0)^a (D_i A_0)^a + (D_i \Phi)^\dagger (D_i \Phi) + \frac{1}{2} m_D^2 A_0^a A_0^a + \frac{1}{4} \lambda_A (A_0^a A_0^a)^2 + m_3^2 \Phi^\dagger \Phi + \lambda_3 (\Phi^\dagger \Phi)^2 + h_3 A_0^a A_0^a \Phi^\dagger \Phi \right\}. \quad (1.6)$$

The 3-dimensional fields have the canonical dimension $(\text{GeV})^{1/2}$, whereas the 3-dimensional couplings have dimension $(\text{GeV})^1$. The parameters in eq. (1.6) have well-defined relations to the 4-dimensional parameters of eq. (1.5) [17]. Here no different notation for the fields is used for convenience.

Since we are interested in the theory at scales $\sim g^2 T$, the mass $m_D \sim gT$ can be viewed as large and one may further simplify the theory by entirely integrating out the A_0 field yielding an effective action

$$S_{\text{eff}}[A_i^a(x), \Phi_i(x)] = \int d^3x \left\{ \frac{1}{4} F_{ij}^a F_{ij}^a + (D_i \Phi)^\dagger (D_i \Phi) + m_3^2 \Phi^\dagger \Phi + \lambda_3 (\Phi^\dagger \Phi)^2 \right\}. \quad (1.7)$$

This is the usual linear $SU(2)$ Higgs model in 3 dimensions. It contains all the infrared physics of the hot electroweak standard model. From now on, we restrict the discussion to 3-dimensional gauge theories. Concerning the mass generating mechanism, we not only choose a Higgs model, but also consider a non-linear σ -model.

We now discuss some properties concerning renormalization which are characteristic for the 3-dimensional Higgs model. The model of eq. (1.7) is super-renormalizable and has three parameters m_3, λ_3 and g_3^2 . There is only a finite number of irreducible UV-divergent graphs, whose topologies are depicted in fig. 1.2. The one-loop diagram is linearly divergent and the two-loop setting-sun diagram contains a logarithmic divergence. All these diagrams correspond to a mass renormalisation, no wave function or coupling constant renormalization is needed in the 3-dimensional theory. In the minimal subtraction scheme \overline{MS} of dimensional regularisation the one-loop diagram is finite. The theory is then finite to one-loop order, at the two-loop level mass counterterms have to be added to the Lagrangian, and to higher orders no additional divergences arise.

1.3 Lattice simulations in the symmetric phase

In this last introductory section, an overview of recent lattice calculations is given, which deal with the physical picture, in particular the mass spectrum of the symmetric phase of the 3-dimensional Higgs model (1.7).

Apart from the motivation to study the 3-dimensional theory as a high temperature effective theory, there are other reasons for looking at 3-dimensional theories instead of the full 4-dimensional finite temperature field theory on the lattice. As a consequence of their super-renormalizability, they exhibit a very good scaling behaviour, so that one can extrapolate results of simulations to the continuum limit much more accurately. 3-dimensional theories can be regarded as laboratories for studying the qualitative features of confinement in QCD.

In spite of intensive research on the lattice, the understanding of the symmetric phase is still incomplete. Philipsen et. al. looked at the mass spectrum by calculating gauge-invariant operators, which lead to a picture of a confining phase with a dense spectrum of bound states [20].

In particular they studied the following correlation functions

$$\begin{aligned} R(x) &= \text{Tr} \left(\Phi^\dagger(x) \Phi(x) \right), \\ L(x) &= \text{Tr} \left((D_\mu \Phi(x))^\dagger D_\mu \Phi(x) \right), \\ P(x) &= \frac{1}{2} \text{Tr} (A_{\mu\nu} A_{\mu\nu}), \end{aligned} \quad (1.8)$$

for scalar states with $J^{PC} = 0^{++}$, while for vector states the standard operator is

$$V_\mu^a(x) = \frac{1}{2} \text{Tr} \left(\Phi^\dagger(x) \overleftrightarrow{D}_\mu \Phi(x) \tau^a \right), \quad (1.9)$$

τ^a being the triplet of Pauli matrices.

Screening masses can be extracted from the corresponding two-point functions with the following results for the symmetric phase

$$\begin{aligned} G_R(x-y) &= \langle R(x)R(y) \rangle \sim e^{-m_R|x-y|}, & m_R &= 0.839(15)g^2 \\ G_V(x-y)_{\mu\nu} &= \langle V_\mu(x)V_\nu(y) \rangle \sim e^{-m_V|x-y|}, & m_V &= 1.27(6)g^2 \\ G_L(x-y) &= \langle L(x)L(y) \rangle \sim e^{-m_L|x-y|}, & m_L &= 1.47(4)g^2 \\ G_P(x-y) &= \langle P(x)P(y) \rangle \sim e^{-m_P|x-y|}, & m_P &= 1.60(4)g^2. \end{aligned} \quad (1.10)$$

Other attempts concentrate directly on the gauge boson propagator. Karsch et. al. [21] calculated the following correlation function for the gauge field on the lattice in Landau gauge,

$$G_W(x-y)_{\mu\nu} = \langle W_\mu(x)W_\nu(y) \rangle \sim e^{-m|x-y|}, \quad (1.11)$$

and obtained a propagator mass for the vector field,

$$m^{(L)} = 0.35(1)g^2. \quad (1.12)$$

At the moment, the only available analytical tool to calculate this propagator mass is via gap equations. This approach is the central point in this thesis, and its concept as well as the corresponding one- and two-loop calculations are extensively discussed in the following chapters. As will be demonstrated, the gap equation yields a mass of about the same size as the fixed gauge simulation of eq. (1.12).

The connection between masses of eq. (1.10) and eq. (1.12) is still an unsolved puzzle. In [22] Buchmüller and Philipsen explain the difference between the gauge-invariant correlations functions and the ones in a fixed gauge. They argue that the two correlation functions are only proportional, if the fluctuations of the Higgs field are small compared to the vacuum expectation value. This is not the case in the symmetric phase, so that one cannot expect that the gauge-dependent two-point functions constitute a good approximation to the gauge-invariant two-point functions. The conjecture is also made that multi-particle states of constituent scalar and vector bosons determine the exponential fall-off of the gauge-invariant two-point functions, since the fluctuations dominate

the hot phase. For G_R this would be a $(\Phi^\dagger\Phi)$ state, for G_L a $(\Phi^\dagger AA\Phi)$ state and for G_V a $(\Phi^\dagger A\Phi)$ state. In addition to these bound states involving the scalar field, there is also a purely gluonic state, a W-ball (AAAA) for G_P . This constituent picture, which interpretes the propagator mass as a constituent mass, could qualitatively explain the measured masses of eq. (1.10). Other bound state models have been considered in [23].

Recently, other non-perturbative, non-local and gauge-invariant operators were investigated on the lattice [24] in order to measure the constituent or screening masses of the bound states and compare them with the mass obtained in gap equations and the Landau gauge simulation. The numerical value extracted for the screening mass M is

$$M \approx 0.73 g^2. \quad (1.13)$$

This is approximately half of the lightest 0^{++} W-ball mass, which was $1.60(4)g^2$, and twice the propagator mass. Unfortunately, this result does not shed much light on the physical interpretation of the propagator mass.

A comparison of the lattice calculations in the Higgs model with the results in the pure gauge theory shows almost no difference between the masses of the W-balls and the glueballs [20,25]. The bound states of scalars seem to be rather disconnected from the W-ball part of the spectrum. This approximate decoupling of the pure gauge sector from the Higgs sector in the symmetric phase is confirmed by the analytical gap equation approach.

Chapter 2

One-loop Gap Equations

In this chapter, the concept of gap equations is discussed. In this framework, it is possible to estimate the size of the dynamically generated mass in a 3-dimensional $SU(2)$ gauge theory analytically. The calculations in several models are reviewed and extended here. We focus on two models in particular, the linear $SU(2)$ Higgs model and the corresponding non-linear σ -model, and concentrate on unitary gauge and renormalization issues.

2.1 Gap equation principles

In chapter 1 we saw that in the high-temperature phase of the standard model a naive perturbative expansion with a vanishing vector boson mass leads to severe infrared divergences in the magnetic sector of the theory. The infrared problem in the electric sector, however, could be solved by a resummation (ring summation). Calculations are done with an effective propagator containing the electric mass which, in contrast to the magnetic mass, is perturbatively calculable (at least to leading order).

Let us follow a similar path for the magnetic mass. In ordinary perturbation theory with a free and interaction part of the action, $S = S_0 + S_I$, one expands in S_I , which is supposed to be small. A resummation of the perturbation theory is obtained by adding and subtracting a mass term in S

$$S_{eff} = S_0 + S_m + S_I - S_m. \quad (2.1)$$

Now, one expands in $S_I - S_m$ and uses an effective tree-level propagator extracted from $S_0 + S_m$. The subtracted term enters the perturbation theory at one loop higher than the added term. This is formalized by introducing a loop-counting parameter l : one rescales all the fields by \sqrt{l} and

calculates with the modified action

$$S_{eff} = \frac{1}{l} \left(S_0(\sqrt{l}W, \sqrt{l}\Phi) + S_m(\sqrt{l}W, \sqrt{l}\Phi) + S_I(\sqrt{l}W, \sqrt{l}\Phi) \right) - S_m(\sqrt{l}W, \sqrt{l}\Phi) \quad (2.2)$$

in a formal l -expansion [41]. Perturbative calculations are no longer done to a fixed order of the gauge coupling g , but as a power series in l , resulting in a rearranged or resummed perturbation series.

The choice of the mass term is at first arbitrary. For our problem, it is required to contain the correction of the self energies to the considered order in perturbation theory. This yields a self-consistent condition for the vector boson mass, which is known as the gap equation. It determines the particular size of the tree-level mass-term $m = Cg^2$, so that the transverse part of the (Euclidean) vector boson propagator remains at $p^2 = -m^2$ to the considered loop-order, i.e.

$$\begin{aligned} D_T(p^2) &= \frac{1}{p^2 + m^2 - \Pi_T(p^2)} \\ &\sim \frac{Z}{p^2 + m^2} \quad \text{for } p^2 \sim -m^2, \end{aligned} \quad (2.3)$$

with some residue Z . With eq. (2.3) one obtains the desired gap equation for the self-energy in resummed perturbation theory

$$\frac{\Pi_T(p^2 = -m^2)}{1 - \frac{\partial \Pi_T}{\partial p^2}(p^2 = -m^2)} = 0. \quad (2.4)$$

In n -th order of resummed perturbation theory one calculates eq. (2.4) up to l^n and solves the gap equation for m . At one-loop eq. (2.4) reduces to

$$\Pi_T^{1\text{-loop}}(p^2 = -m^2) = 0. \quad (2.5)$$

and to two loops it reads,

$$\Pi_T(p^2 = -m^2) \left(1 + \frac{\partial \Pi_T}{\partial p^2}(p^2 = -m^2) \right) = 0. \quad (2.6)$$

In theories with a BRS-symmetry the position of the pole of the propagator and therefore eq. (2.4) is gauge-independent on mass-shell [26]. The self-energy itself is not gauge-invariant on mass-shell except at the one-loop level.

2.2 The $SU(2)$ Higgs model

Let us start with the 3-dimensional $SU(2)$ Higgs model as motivated in chapter 1. It is defined by the action

$$S = \int d^3x \text{Tr} \left[\frac{1}{2} W_{\mu\nu} W_{\mu\nu} + (D_\mu \Phi)^\dagger D_\mu \Phi + \mu^2 \Phi^\dagger \Phi + 2\lambda (\Phi^\dagger \Phi)^2 \right], \quad (2.7)$$

with

$$\Phi = \frac{1}{2} (\sigma + i\vec{\pi} \cdot \vec{\tau}), \quad D_\mu \Phi = (\partial - igW_\mu) \Phi, \quad W_\mu = \frac{1}{2} \vec{\tau} \cdot \vec{W}_\mu. \quad (2.8)$$

Here \vec{W}_μ is the vector field, σ is the Higgs field, $\vec{\pi}$ is the Goldstone boson field and $\vec{\tau}$ the triplet of Pauli matrices.

Varying μ^2/g^4 one expects a phase transition which is of first order for sufficiently small values of λ/g^2 . It is known that the Higgs phase and the symmetric phase are analytically connected [27]. It is therefore conceivable that the Higgs model has a simpler structure than the pure gauge theory.

We are interested in the Higgs and vector boson masses in both phases which determine the exponential fall-off of the corresponding two-point functions at large separation $|x - y|$,

$$\begin{aligned} \langle \sigma(x) \sigma(y) \rangle &\sim e^{-M|x-y|}, \\ \langle W_\mu(x) W_\mu(y) \rangle &\sim e^{-m|x-y|}. \end{aligned} \quad (2.9)$$

In the Higgs phase, these 2-point functions can be evaluated in perturbation theory. The masses m and M are given by the gauge-independent poles of the corresponding propagators in momentum space.

In (2.7) we shift the Higgs field σ around its vacuum expectation value $v, \sigma = v + \sigma'$, add an R_ξ -gauge fixing term and the corresponding ghost terms,

$$\begin{aligned} \mathcal{L}_{GF} &= \frac{1}{2\xi} \left(\partial_\mu W_\mu^a - \xi \frac{g}{2} v \pi^a \right)^2, \\ \mathcal{L}_{FP} &= -c^{*a} \left(\partial^2 - \epsilon^{abc} \partial_\mu W_\mu^c - \xi \frac{g^2}{4} v \left(v + \sigma' - \epsilon^{abc} \pi^c \right) \right) c^a. \end{aligned} \quad (2.10)$$

This yields the following masses for the vector boson and the Higgs field,

$$m_0^2 = \frac{g^2}{4} v^2, \quad M_0^2 = \mu^2 + 3\lambda v^2. \quad (2.11)$$

The ghost and Goldstone boson mass is given by $\sqrt{\xi} m_0$.

In order to extract a non-vanishing mass in the symmetric phase, where in ordinary perturbation theory $v = 0$, we apply the idea of resummation developed in the last section. The tree-level masses m_0^2 and M_0^2 are expressed as

$$m_0^2 = m^2 - \delta m^2, \quad M_0^2 = M^2 - \delta M^2, \quad (2.12)$$

where m and M enter the propagators of the loop expansion, and δm^2 and δM^2 are treated perturbatively as counter-terms. For a gauge-invariant one-loop gap equation it is necessary and sufficient to have a BRS-invariant resummed tree-level action. This requires a suitable resummation of the ghost and Goldstone boson mass as well as of the following vertices,

$$\begin{aligned} \frac{g^2 v}{2} &= gm - \delta V^g, \\ \lambda v &= \frac{gM}{4m} - \delta V^{\lambda v}, \\ \lambda &= \frac{g^2 M^2}{8m^2} - \delta V^\lambda. \end{aligned} \quad (2.13)$$

After these steps, one arrives at the Lagrangian,

$$\begin{aligned} \mathcal{L} &= \mathcal{L}_R + \mathcal{L}_1 + \mathcal{L}_0, \\ \mathcal{L}_R &= \frac{1}{4} \vec{W}_{\mu\nu} \vec{W}_{\mu\nu} + \frac{1}{2\xi} \left(\partial_\mu \vec{W}_\mu \right)^2 + \frac{1}{2} m^2 \vec{W}_\mu^2 \\ &\quad + \frac{1}{2} (\partial_\mu \sigma')^2 + \frac{1}{2} M^2 \sigma'^2 + \frac{1}{2} (\partial_\mu \vec{\pi})^2 + \frac{\xi}{2} m^2 \vec{\pi}^2 \\ &\quad + \frac{g}{2} m \sigma' \vec{W}_\mu^2 + \frac{g}{2} \vec{W}_\mu \cdot (\vec{\pi} \partial_\mu \sigma' - \sigma' \partial_\mu \vec{\pi}) + \frac{g}{2} (\vec{W}_\mu \times \vec{\pi}) \cdot \partial_\mu \vec{\pi} \\ &\quad + \frac{g^2}{8} \vec{W}_\mu^2 (\sigma'^2 + \vec{\pi}^2) + \frac{g}{4} \frac{M^2}{m} \sigma' (\sigma'^2 + \vec{\pi}^2) + \frac{g^2}{32} \frac{M^2}{m^2} (\sigma'^2 + \vec{\pi}^2)^2 \\ &\quad + \partial_\mu c^{\bar{a}} \partial_\mu c^a + \xi m^2 c^{\bar{a}} c^a \\ &\quad + g \partial_\mu c^{\bar{a}} \cdot (\vec{W}_\mu \times c^{\bar{a}}) + \xi \frac{g}{2} m \sigma' c^{\bar{a}} c^a + \xi \frac{g}{2} m c^{\bar{a}} \cdot (\vec{\pi} \times c^{\bar{a}}) \\ \mathcal{L}_1 &= -\delta m^2 \left(\frac{1}{2} \vec{W}_\mu^2 + \frac{\xi}{2} \vec{\pi}^2 + \xi c^{\bar{a}} c^a \right) - \frac{1}{2} \delta M^2 \sigma'^2 + \frac{1}{2} (\mu^2 + \lambda v^2) \vec{\pi}^2 \\ &\quad + v (\mu^2 + \lambda v^2) \sigma' - \frac{1}{2} \delta V^g \left(\sigma' \vec{W}_\mu^2 + \xi \sigma' c^{\bar{a}} c^a + \xi c^{\bar{a}} \cdot (\vec{\pi} \times c^{\bar{a}}) \right) \end{aligned}$$

$$\begin{aligned}
& -\delta V^{\lambda\nu} \sigma' (\sigma'^2 + \vec{\pi}^2) - \frac{1}{4} \delta V^\lambda (\sigma'^2 + \vec{\pi}^2)^2, \\
\mathcal{L}_0 &= \frac{1}{2} \mu^2 v^2 + \frac{1}{4} \lambda v^4.
\end{aligned} \tag{2.14}$$

In resummed perturbation theory, the vertices defined by \mathcal{L}_1 are treated as counter-terms. The propagators for the vector boson, Goldstone boson, ghost and Higgs boson, respectively, are easily obtained,

$$\begin{aligned}
D_{\mu\nu}^{ab}(p) &= \delta_{ab} \frac{1}{p^2 + m^2} \left(\delta_{\mu\nu} + (\xi - 1) \frac{p_\mu p_\nu}{p^2 + \xi m^2} \right), \\
\Delta_\pi^{ab}(p) &= \Delta_c^{ab}(p) = \frac{\delta_{ab}}{p^2 + \xi m^2}, \\
\Delta_\sigma^{ab}(p) &= \frac{1}{p^2 + M^2}.
\end{aligned} \tag{2.15}$$

The coupled set of gap equations for the Higgs boson and vector boson masses then reads [28],

$$\begin{aligned}
\delta m^2 + \Pi_T(p^2 = -m^2) &= 0, \\
\delta M^2 + \Sigma(p^2 = -M^2) &= 0, \\
\langle \sigma' \rangle &= 0,
\end{aligned} \tag{2.16}$$

where Σ is the one-loop Higgs boson self-energy and Π_T is the transverse part of the vacuum polarization tensor,

$$\Pi_{\mu\nu}^{ab}(p) = \delta_{ab} \left[\left(\delta_{\mu\nu} - \frac{p_\mu p_\nu}{p^2} \right) \Pi_T(p^2) + \frac{p_\mu p_\nu}{p^2} \Pi_L(p^2) \right]. \tag{2.17}$$

The results for the self-energies in R_ξ -gauge can be found in [28]. Here the expressions in unitary gauge, $\xi \rightarrow \infty$, are given. A peculiarity of the unitary gauge is that the limit $\xi \rightarrow \infty$ must be performed before divergent integrals are evaluated [29]. Otherwise one would get an infinite result for Π_T . This and some more characteristics of the unitary gauge are discussed in detail in section 2.4. For the moment, we just state that a separate calculation has to be made in unitary gauge. For the one-loop self-energy all the diagrams including Goldstone and ghost lines, which become infinitely heavy, can be left out. The tree-level propagator for the vector boson changes to

$$D_{\mu\nu}^{ab}(p) = \delta_{ab} \frac{1}{p^2 + m^2} \left(\delta_{\mu\nu} + \frac{p_\mu p_\nu}{m^2} \right). \tag{2.18}$$

The calculation in unitary gauge yields for the self-energies

$$\begin{aligned}
\Pi_T^{\xi=\infty}(p^2) = g^2 & \left[\frac{m}{gM^2} v (\mu^2 + \lambda v^2) + \left(\frac{p^4}{4m^4} - \frac{p^2}{m^2} - \frac{15}{8} + \frac{3m^2}{M^2} - \frac{m^2}{8p^2} + \frac{M^2}{8p^2} \right) A_0(m^2) \right. \\
& + \left(\frac{5}{8} - \frac{M^2}{8p^2} + \frac{m^2}{8p^2} \right) A_0(M^2) \\
& - \left(\frac{p^6}{8m^4} - \frac{p^4}{m^2} - 5p^2 + 4m^2 \right) B_0(p^2, m^2, m^2) \\
& \left. + \left(\frac{m^2}{2} - \frac{1}{8p^2} (p^2 + M^2 - m^2)^2 \right) B_0(p^2, m^2, M^2) \right],
\end{aligned} \tag{2.19}$$

and

$$\begin{aligned}
\Sigma^{\xi=\infty}(p^2) = g^2 & \left[\frac{m}{gM^2} v (\mu^2 + \lambda v^2) + \left(\frac{p^4}{4m^4} - \frac{p^2}{m^2} - \frac{15}{8} + \frac{3m^2}{M^2} - \frac{m^2}{8p^2} + \frac{M^2}{8p^2} \right) A_0(m^2) \right. \\
& + \left(\frac{5}{8} - \frac{M^2}{8p^2} + \frac{m^2}{8p^2} \right) A_0(M^2) \\
& - \left(\frac{p^6}{8m^4} - \frac{p^4}{m^2} - 5p^2 + 4m^2 \right) B_0(p^2, m^2, m^2) \\
& \left. + \left(\frac{m^2}{2} - \frac{1}{8p^2} (p^2 + M^2 - m^2)^2 \right) B_0(p^2, m^2, M^2) \right].
\end{aligned} \tag{2.20}$$

Here A_0 and B_0 are the 3-dimensional integrals,

$$\begin{aligned}
A_0(m^2) &= \int \frac{d^3k}{(2\pi)^3} \frac{1}{k^2 + m^2}, \\
B_0(p^2, m_1^2, m_2^2) &= \int \frac{d^3k}{(2\pi)^3} \frac{1}{(k^2 + m_1^2) ((k+p)^2 + m_2^2)}.
\end{aligned} \tag{2.21}$$

In dimensional regularization they turn out to be finite. For explicit formulae see appendix A. The on-shell self-energies in unitary gauge coincide with the self-energies in R_ξ -gauge for arbitrary ξ .

One more comment has to be made concerning the third equation of (2.16), which determines the vacuum expectation value v of the Higgs field self-consistently. As v is no physical observable, this equation is not gauge parameter independent. On the other hand, the masses obtained from the gap equations (2.16) are physical observables and must therefore be gauge independent. The weak gauge dependence induced by the gauge dependence of v has to be cancelled at higher orders.

Details of the calculation and the solutions of the gap equations in the linear Higgs model can be found in [28]. The main result is that deeply in the symmetric phase, the value for the gap mass is approximately the same as the one obtained in a non-linear σ model, which requires the evaluation of much less diagrams than in the linear model. That is why we concentrate on the simpler non-linear model first when calculating two-loop effects. It is introduced in the following section.

2.3 The non-linear σ -model

We start from the Higgs model before resummation. To obtain the non-linear σ -model, one eliminates one degree of freedom by the constraint

$$\sigma^2 = v^2 - \pi^2, \quad (2.22)$$

and takes the limit $\lambda, \mu \rightarrow \infty$. Resumming the masses for the vector boson, Goldstone boson and ghost, and supplementing these mass redefinitions by resummation of the vertices involving v as in the linear Higgs model, one arrives at the following Lagrangian. Note, that we have neglected all higher-dimensional operators which do not contribute to the two-loop self-energy.

$$\begin{aligned} \mathcal{L} &= \mathcal{L}_R + \mathcal{L}_1, \\ \mathcal{L}_R &= \frac{1}{4} \vec{W}_{\mu\nu} \vec{W}_{\mu\nu} + \frac{1}{2\xi} (\partial_\mu \vec{W}_\mu)^2 + \frac{1}{2} m^2 \vec{W}_\mu^2 \\ &\quad + \frac{1}{2} (\partial_\mu \vec{\pi})^2 + \frac{\xi}{2} m^2 \vec{\pi}^2 + \frac{g}{2} (\vec{W}_\mu \times \vec{\pi}) \\ &\quad + \partial_\mu \vec{c}^\dagger \partial_\mu \vec{c} + \xi m^2 \vec{c}^\dagger \vec{c} \\ &\quad + g \partial_\mu \vec{c}^\dagger \cdot (\vec{W}_\mu \times \vec{c}) + \xi \frac{g}{2} m \vec{c}^\dagger \cdot (\vec{\pi} \times \vec{c}) \\ &\quad + \frac{g^2}{8} \frac{(\vec{\pi} \partial_\mu \vec{\pi})^2}{m^2} - \frac{g^2}{4} \vec{W}_\mu \cdot \vec{\pi} \frac{\partial_\mu \vec{\pi}}{m} + \frac{g^2}{8} \vec{W}_\mu \cdot \partial_\mu \vec{\pi} \frac{\vec{\pi}^2}{m} \\ &\quad - \xi \frac{g^2}{8} \vec{\pi}^2 \vec{c}^\dagger \vec{c} \\ \mathcal{L}_1 &= -\delta m^2 \left(\frac{1}{2} \vec{W}_\mu^2 + \frac{\xi}{2} \vec{\pi}^2 + \xi \vec{c}^\dagger \vec{c} \right), \end{aligned} \quad (2.23)$$

Again the terms from \mathcal{L}_1 are treated as counter-terms. δm^2 is the same as in the linear model. We solve the gap equation in the limit $v = 0$. If we get a non-zero value for m , a vector boson mass

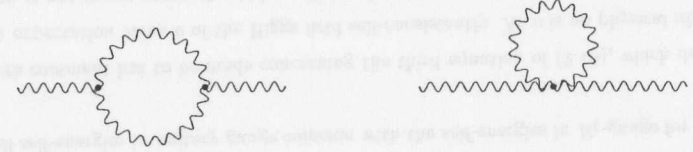


Figure 2.1: Diagrams contributing to the one-loop gap equation in the unitary gauge

is dynamically generated in the symmetric phase.

In unitary gauge the unphysical degrees of freedom decouple and one is left with a massive Yang-Mills theory. In this case, the calculation of the vector boson self-energy involves only two diagrams (see fig. 2.1), yielding [41]

$$\begin{aligned} \Pi_T^{\xi=\infty}(p^2) &= g^2 \left[\left(\frac{p^4}{4m^4} - 2 - \frac{p^2}{m^2} \right) A_0(m^2) \right. \\ &\quad \left. - \left(\frac{p^6}{8m^4} - \frac{p^4}{m^2} - 5p^2 + 4m^2 \right) B_0(p^2, m^2, m^2) \right] \\ &= -\frac{g^2 m}{16\pi} \left(\frac{63}{4} \ln 3 - \frac{3}{4} \right), \end{aligned} \quad (2.24)$$

This result agrees with the one for arbitrary finite ξ , which can be found in [30] on mass-shell, since the tree-level resummed action of the non-linear model is BRS-invariant. As expected, the longitudinal part of the polarization tensor vanishes for all p^2 . The gauge-invariant gap equation of the non-linear σ -model,

$$m^2 = \frac{g^2 m}{16\pi} \left(\frac{63}{4} \ln 3 - \frac{3}{4} \right), \quad (2.25)$$

has a finite and positive solution

$$m_{SM}^2 \simeq 0.28g^2, \quad (2.26)$$

which is in good agreement with the lattice result of Karsch et. al. (1.12).

In the non-linear σ -model there are non-renormalizable vertices. At one-loop level there is no problem with renormalizability in dimensional regularization, as in this scheme all one-loop integrals are finite in 3 dimensions. How to deal with the divergences at two-loops will be discussed in later chapters.

2.4 Peculiarities of the unitary gauge

As already indicated, the unitary gauge has to be treated with care. It has the advantage, that loop calculations may be simpler than in R_ξ -gauge because there are less Feynman diagrams to be considered. On the other hand, the resulting expressions may be more complex because of the form of the vector boson propagator which is proportional to the zeroth instead of the inverse second power of the energy. As a consequence of this bad high-energy behaviour one loses renormalizability [31].

In the Higgs model one obtains the unitary gauge either by performing the limit in each diagram before evaluating divergent integrals or by integrating out the unphysical fields (Goldstone boson and ghosts) in the Lagrangian, which get infinite masses and decouple. The ghost-ghost-scalar coupling becomes infinite, too, so that the ghost term does not completely vanish: there remains a quartic divergent, i. e. proportional to $\delta^4(0)$, non-polynomial Higgs-self-coupling term [32]. This term can be set to zero in dimensional regularization [33].

However, other difficulties arise when performing unitary gauge calculations in connection with dimensional regularization. Let us look at the simplest one-loop integral in 3 dimensions,

$$A_0(m^2) = \int \frac{d^3k}{(2\pi)^3} \frac{1}{k^2 + m^2}, \quad (2.27)$$

which reads in dimensional regularization and in cutoff-regularization, respectively,

$$\begin{aligned} A_0^{DR}(m^2) &= -\frac{m}{4\pi} \\ A_0^\Lambda(m^2) &= \frac{1}{2\pi^2} \left(\Lambda - m \arctan \frac{\Lambda}{m} \right) \\ &\stackrel{\Lambda \rightarrow \infty}{\approx} \frac{\Lambda}{2\pi^2} + A_0^{DR}(m^2). \end{aligned} \quad (2.28)$$

If the mass of the internal particle becomes infinite, A_0 should be zero, as it is indeed the case in cutoff-regularization. In dimensional regularization, however, performing the limit $m \rightarrow \infty$ after integration yields $A_0 \rightarrow \infty$. To get the correct answer in a unitary gauge calculation in dimensional regularization, one has to take the limit $\xi \rightarrow \infty$ *before* divergent integrals are evaluated.

Let us now discuss renormalizability in the unitary gauge. In dimensional regularization all one-loop n -point integrals are finite in 3 dimensions. Using this scheme, the gap equation has to be renormalized only at the two-loop level. In cutoff-regularization, however, A_0 is manifestly linearly divergent, requiring a renormalization of the gap equation already at one loop.

To go into details, consider the vector boson self-energy in unitary gauge of the non-linear σ -model in cutoff-regularization. The result is

$$\Pi_T^{\xi \rightarrow \infty}(q^2) = g^2 \left(-\frac{4}{3} - \frac{19}{15} \frac{q^2}{m^2} + \frac{1}{3} \frac{q^4}{m^4} \right) \frac{\Lambda}{2\pi^2} + \Pi_T^{\xi \rightarrow \infty}(q^2) \Big|_{DR}. \quad (2.29)$$

Notice the high powers in the external momentum in front of Λ , which cannot be removed by the usual redefinition of parameters in the Lagrangian. This is a consequence of the high-energy behaviour of the propagator in unitary gauge, it is not due to the non-renormalizability of the non-linear σ -model. Even in renormalizable theories one would obtain these high powers of q^2 .

For comparison, the self-energy in renormalizable gauges, i. e. for arbitrary finite ξ , reads

$$\Pi_T^\xi(q^2) = -g^2 \frac{\Lambda}{6\pi^2} + \Pi_T^\xi(q^2) \Big|_{DR}. \quad (2.30)$$

Here, only a gauge-independent mass renormalization is needed, as is already suggested by naive power counting. After performing this renormalization, the gap equation in cut-off regularization of the non-linear σ -model is identical to the one in dimensional regularization, since the on-shell finite part is the same in both schemes.

2.5 Other one-loop calculations

In recent years, other one-loop calculations have been performed. They all start from a massless Yang-Mills theory, then add and subtract some gauge-invariant mass-term. One could also view the calculation of section 2.3 in a resummed non-linear σ -model as one in a resummed pure gauge theory if one slightly modifies the resummation scheme: one adds and subtracts the whole σ -model, not just the masses. At the one-loop level this leads to the same gap equation as before.

Using this modified resummation scheme, it is possible to integrate out the Goldstone and ghost fields exactly in an arbitrary gauge, provided one uses a gauge-fixing term which depends only on W_μ [41]. For more details see chapter 4.

Let us briefly review the other gap equation approaches for the 3-dimensional $SU(2)$ gauge theory. Alexanian and Nair considered a gap equation based on the Chern-Simons eikonal [34]. Interestingly, their one-loop gap equation yields a magnetic mass closely related to m_{SM} ,

$$m_{AN} = \frac{4}{3} m_{SM} \simeq 0.38 g^2. \quad (2.31)$$

Jackiw and Pi considered the non-local action

$$S_m^{(JP)} = m^2 \text{Tr} \int d^3x F_\mu \frac{1}{D^2} F_\mu, \quad (2.32)$$

where $F_\mu = \frac{1}{2}\epsilon_{\mu\nu\rho}F_{\nu\rho}$ [35] and obtained a complex magnetic mass with the mass term of eq. (2.32), which however can be modified such that the generated mass becomes real. Another attempt was recently made by Cornwall [36]. He used the pinch-technique in a non-linear σ -model in order to obtain a self-energy which is gauge parameter independent for all external momenta, not just on mass-shell. His pinch-technique gap equation lead to a gap mass ¹ of

$$m_C \simeq 0.25g^2. \quad (2.33)$$

Chapter 3

Calculation Techniques for Two-loop Propagator Integrals

Before extending the gap equation approach to two loops, we discuss a newly constructed method for reducing two-loop self-energy type integrals of Feynman diagrams to a set of basic integrals. It has recently been developed by O. Tarasov [37].

As in our case all propagators are massive and the external momentum does not vanish, the reduction of the scalar integrals to basic integrals with no momenta in the numerators turns out to be the most difficult step in the two-loop calculation. Using Tarasov's recurrence relations it is possible to reduce the self-energy integrals to a small set of linearly independent basic integrals. For the first time this method arrives at a complete reduction and stays on an algebraic level as far as possible.

In this chapter, we look at the algorithm in more detail. We discuss the whole formalism in Minkowski space, contrary to all other chapters of this thesis, in order to be easily comparable to the work of Tarasov.

3.1 The concept of reducing scalar integrals to basic integrals

There have recently been other attempts in the literature to build an algorithm for the complete reduction of two-loop integrals with arbitrary masses to basic integrals. The earlier approach developed in [38] has some disadvantages: first, it is not a complete reduction, i. e. the basic integrals are not linearly independent, and second, using MATHEMATICA it is not able to handle the huge expressions, which appear in two-loop self-energies for vector bosons in a non-abelian

¹In our opinion, it is not clear why m_C and m_{SM} are not identical, since the diagrams which are added in the pinch-technique formalism usually vanish on mass-shell.

gauge theory. The method of Tarasov, however, does not show these deficits. We checked his formulae and implemented them into a FORM [39] package.

Let us sketch the basic features of this program and show in simple examples how the reduction mechanism works. The method used here is only applicable in dimensional regularization. If we calculate transverse or longitudinal parts of self-energies, all two-loop Feynman diagrams yield expressions of the form

$$I^d(q^2) = \frac{1}{\pi^d} \int \int d^d k_1 d^d k_2 \frac{f(k_1^2, k_2^2, k_1 q, k_2 q, k_1 k_2)}{c_1^{\nu_1} c_2^{\nu_2} c_3^{\nu_3} c_4^{\nu_4} c_5^{\nu_5}}, \quad (3.1)$$

f being a polynomial in its arguments and c_i being inverse propagators in Minkowski space,

$$\begin{aligned} c_1 &= k_1^2 - m_1^2 + i\epsilon, & c_2 &= k_2^2 - m_2^2 + i\epsilon \\ c_3 &= (k_1 - q)^2 - m_3^2 + i\epsilon, & c_4 &= (k_2 - q)^2 - m_4^2 + i\epsilon \\ c_5 &= (k_1 - k_2)^2 - m_5^2 + i\epsilon. \end{aligned} \quad (3.2)$$

The causal $i\epsilon$'s will be omitted for brevity from now on. At first we apply substitutions of the form

$$\frac{2k_1 k_2}{c_5} = 1 - \frac{k_1^2 + k_2^2 - m_5^2}{c_5}, \quad (3.3)$$

and analogous relations for $\frac{k_2 q}{c_4}$, $\frac{k_1 q}{c_3}$, $\frac{k_2^2}{c_2}$ and $\frac{k_1^2}{c_1}$. As a next step, similar simplifications are done for the remaining $\frac{k_1^2}{c_3}$ as well as for $\frac{k_2^2}{c_4}$. After all these algebraic manipulations the remaining integrals with irreducible numerators contain the scalar products $k_1 q$ and $k_2 q$. They can be written as a combination of scalar integrals with shifted space-time dimension and higher powers of the propagators as shown in the following simple example.

$$I_{\text{example}}^d(q^2) = \frac{1}{\pi^d} \int \int d^d k_1 d^d k_2 \frac{(k_1 q)^2}{c_1 c_2 c_5}, \quad (3.4)$$

where all the masses are taken to be equal for simplicity. Introducing an auxiliary scalar parameter β by

$$k_1 q = \frac{\partial}{i\partial\beta} e^{i\beta k_1 q} \Big|_{\beta=0}, \quad (3.5)$$

using the well-known α -parametric representation of the propagator,

$$\frac{1}{(k^2 - m^2 + i\epsilon)^\nu} = \frac{1}{i^\nu \Gamma(\nu)} \int_0^\infty d\alpha \alpha^{\nu-1} \exp[i\alpha(k^2 - m^2 + i\epsilon)], \quad (3.6)$$

and the d -dimensional Gaussian integration formula,

$$\int d^d k \exp[i(Ak^2 + 2(pk))] = i \left(\frac{\pi}{iA}\right)^{\frac{d}{2}} \exp\left[-\frac{ip^2}{A}\right]. \quad (3.7)$$

we arrive at

$$I_{\text{example}}^d(q^2) = i^{-d} \int \int \int d\alpha_1 d\alpha_2 d\alpha_3 q^2 \frac{\alpha_3}{(\alpha_1 \alpha_2 + \alpha_1 \alpha_3 + \alpha_2 \alpha_3)^{\frac{d+2}{2}}}. \quad (3.8)$$

With the same manipulations we get a relation for an integral in $d+2$ dimensions and with one of the propagators squared,

$$\frac{1}{\pi^{d+2}} \int \int d^d k_1 d^d k_2 \frac{1}{c_1 c_2 c_5^2} = -i^{-d-2} \int \int \int d\alpha_1 d\alpha_2 d\alpha_3 \frac{\alpha_3}{(\alpha_1 \alpha_2 + \alpha_1 \alpha_3 + \alpha_2 \alpha_3)^{\frac{d+2}{2}}}. \quad (3.9)$$

Comparing this with the previous equation leads to the desired result,

$$I_{\text{example}}^d(q^2) = \frac{q^2}{\pi^{d+2}} \int \int d^{d+2} k_1 d^{d+2} k_2 \frac{1}{c_1 c_2 c_5^2}. \quad (3.10)$$

This mechanism works for all integrals with the irreducible numerators $k_1 q$ and $k_2 q$. We are left with integrals having higher space-time dimension and higher powers of the propagators, but without any scalar products in the numerator. The next task is to relate these integrals to integrals with lowest possible powers of the propagators and the generic dimension d by using recurrence relations. These will be introduced in the next section.

3.2 Recurrence relations

In this section we explicitly derive the recurrence relations for two-loop bubble integrals. For simplicity we set all masses equal to m and use the abbreviation

$$I_{\nu_1 \nu_2 \nu_3}^d = \frac{1}{\pi^d} \int \int d^d k_1 d^d k_2 \frac{1}{c_1^{\nu_1} c_2^{\nu_2} c_5^{\nu_3}}. \quad (3.11)$$

In particular we aim at a relation which reduces the power of one of the the propagators by 1 and another relation which reduces the space-time dimension by 2. To obtain a relation, which reduces the power of the propagators, we use partial integration. In particular we look at

$$\int \int d^d k_1 d^d k_2 \left(\frac{\partial}{\partial k_{1\mu}} + \frac{\partial}{\partial k_{2\mu}} \right) \frac{k_{1\mu}}{c_1^{\nu_1} c_2^{\nu_2} c_5^{\nu_3}} = 0. \quad (3.12)$$

Keeping the scalar product $k_1 k_2$ untouched, we get:

$$\frac{\nu_3}{\pi^d} \int \int d^d k_1 d^d k_2 \frac{k_1 k_2}{c_1^{\nu_1} c_2^{\nu_2+1} c_5^{\nu_5}} + m^2 I_{\nu_1+1 \nu_2 \nu_5}^d - \left(\frac{d}{2} - \nu_1\right) I_{\nu_1 \nu_2 \nu_5}^d = 0. \quad (3.13)$$

Reducing the first term by applying eq. (3.3), we get the desired recurrence relation for lowering the power of one of the propagators by one, keeping the dimension d constant,

$$I_{\nu_1+1 \nu_2 \nu_5}^d = I_{\nu_1 \nu_2+1 \nu_5}^d = I_{\nu_1 \nu_2 \nu_5+1}^d = \frac{d-3}{3m^2} I_{\nu_1 \nu_2 \nu_5}^d. \quad (3.14)$$

This equation enables us to reduce each power of the propagators in the two-loop bubble integrals down to one, leaving us only with I_{111}^{d+2n} , which we now seek to reduce now to I_{111}^d . The first term in eq. (3.13) can also be treated in a similar way as the integral in eq. (3.4). We write

$$k_1 k_2 = -\delta_{\mu\nu} \frac{\partial}{\partial a_{1\mu}} \frac{\partial}{\partial a_{2\nu}} e^{i(a_1 k_1 + a_2 k_2)} \Big|_{a_i=0}, \quad (3.15)$$

and apply the same techniques as in the last section arriving at

$$\frac{1}{\pi^d} \int \int d^d k_1 d^d k_2 \frac{k_1 k_2}{c_1^2 c_5^2} = \frac{1}{2} d I_{122}^{d+2}. \quad (3.16)$$

Substituting this into eq. (3.13) we obtain

$$d I_{122}^{d+2} + 2m^2 I_{211}^d - (d-2) I_{111}^d = 0. \quad (3.17)$$

Repeated use of eq. (3.16) leads to the recurrence relation connecting bubble integrals of different space-time dimension with equal powers of the propagators,

$$d(d-1) I_{111}^{d+2} = 3m^2 (m^2 I_{111}^d + I_{110}^d). \quad (3.18)$$

Now we are able to reduce integrals of the type $I_{\nu_1 \nu_2 \nu_5}^{d+2n}$, which we get after the procedure of the previous section, to one basic bubble integral I_{111}^d (plus products of one loop integrals). In our FORM package, we also include relations like eq. (3.17), reducing running times compared to a repeated application of eq. (3.14) and (3.18).

All other two-loop propagator integrals with non-vanishing external momentum and arbitrary masses can be treated in the same way as described above. One should not forget that this technique is only valid for dimensionally regularized integrals. For example, eq. (3.12) requires translational invariance of dimensionally regularized integrals in k -space.

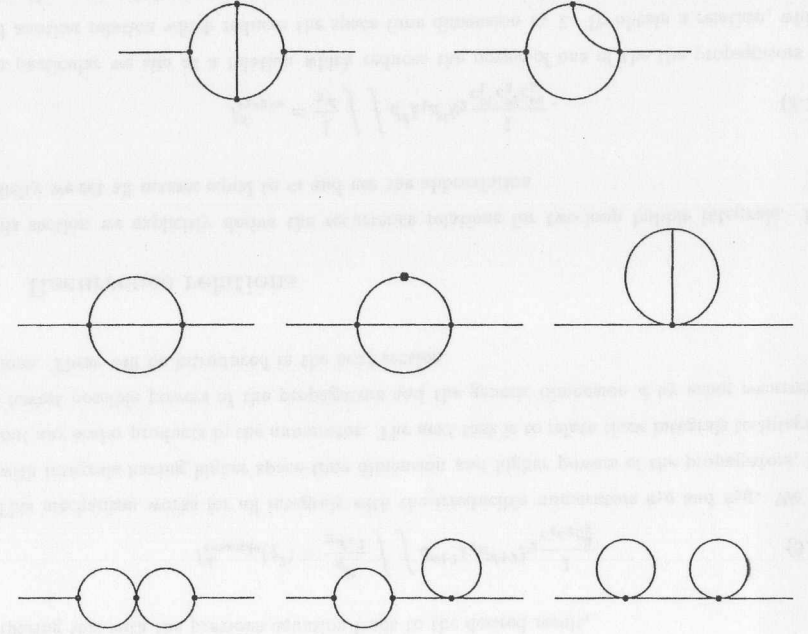


Figure 3.1: Basic integrals for two-loop self-energies

O. Tarasov derived recurrence relations for all two-loop propagator integrals. When checking his equations, only one non-trivial misprint was found. In eq. (67) of [37] there should not be an overall minus sign on the RHS. His method enables us to reduce these integrals to the set of basic two-loop integrals given in fig. 3.1. The dotted propagator means a squared propagator in the integral.

Switching back to Euclidean space, we define

$$F(m_1, m_2, m_3, m_4, m_5) = \int \int \frac{d^d k_1}{(2\pi)^d} \frac{d^d k_2}{(2\pi)^d} \frac{1}{(k_1^2 + m_1^2)(k_2^2 + m_2^2)} \\ \frac{1}{((k_1 - q)^2 + m_3^2)((k_2 - q)^2 + m_4^2)((k_1 - k_2)^2 + m_5^2)}, \\ V(m_1, m_2, m_3, m_4) = \int \int \frac{d^d k_1}{(2\pi)^d} \frac{d^d k_2}{(2\pi)^d} \frac{1}{(k_2^2 + m_1^2)((k_1 - q)^2 + m_2^2)}$$

$$\begin{aligned}
I_{111}(q^2)(m_1, m_2, m_3) &= \frac{1}{((k_2 - q)^2 + m_3^2) ((k_1 - k_2)^2 + m_4^2)}, \\
I_{111}(q^2)(m_1, m_2, m_3) &= \int \int \frac{d^d k_1}{(2\pi)^d} \frac{d^d k_2}{(2\pi)^d} \frac{1}{(k_1^2 + m_1^2) ((k_2 - q)^2 + m_2^2)}, \\
I_{211}(m_1, m_2, m_3) &= -\frac{\partial}{\partial m_1^2} I_{111}(q^2)(m_1, m_2, m_3), \\
I_{121}(m_1, m_2, m_3) &= -\frac{\partial}{\partial m_2^2} I_{111}(q^2)(m_1, m_2, m_3), \\
I_{112}(m_1, m_2, m_3) &= -\frac{\partial}{\partial m_3^2} I_{111}(q^2)(m_1, m_2, m_3), \\
I_{111}(0)(m_1, m_2, m_3) &= \int \int \frac{d^d k_1}{(2\pi)^d} \frac{d^d k_2}{(2\pi)^d} \frac{1}{(k_1^2 + m_1^2) (k_2^2 + m_2^2) ((k_1 - k_2)^2 + m_3^2)}. \quad (3.19)
\end{aligned}$$

The one-loop integrals A_0 and B_0 were already introduced in eq. (2.21).

Apart from the master integral $F(m_1, m_2, m_3, m_4, m_5)$, which has to be evaluated numerically, there exist analytic expressions for the basic integrals in $d = 3 - 2\epsilon$ dimensions [40]. The results are summarized in appendix C. For F a one-dimensional integral remains. In appendix E we evaluate $F(m_1, m_2, m_3, m_4, m_5)$ numerically for some special mass cases.

Chapter 4

Two-loop Gap Equation in the Non-linear σ -model

In this chapter, we extend the method of gap equations to two loops. We start with the non-linear σ -model, as already motivated in section 2.2. There it was shown that deeply in the symmetric phase the solution of the one-loop gap equations in the non-linear model provides a very good approximation to the one-loop gap mass of the linear Higgs model. The two-loop calculation in the linear model, which involves the evaluation of many more diagrams than in the non-linear model, is only justified, if the simpler non-linear case yields a reasonable value for the two-loop gap mass. That this is indeed the case, is shown in the following.

4.1 Further simplifications of the model

In section 2.3, we resummed the masses of the vector boson, Goldstone boson and ghost. Let us look at a slightly modified resummation scheme introduced in section 2.5, which to one loop is equivalent. We add a gauged non-linear σ -model to a pure Yang-Mills theory and subtract the whole σ -model again (including the kinetic term and vertices). To all orders in perturbation theory this describes a pure Yang-Mills theory, whereas the models in section 2.2 and 2.3 represent a linear Higgs and non-linear σ -model, respectively, to all orders. The functional integral for the partition function in this case, where $S_m = S_\sigma$, reads

$$Z = \int DW D\pi \Delta \exp - \frac{1}{l} (S_G + S_\sigma + S_{GF} - lS_\sigma). \quad (4.1)$$

S_G is the massless Yang-Mills action, S_σ the action of the non-linear σ -model, S_{GF} is some gauge-fixing term which depends only on W_μ , and Δ the corresponding Fadeev-Popov determinant. The non-linear σ -model Lagrangian can be written in a compact way

$$\mathcal{L}_\sigma = \langle (\partial_\mu \Phi + A_\mu \Phi)^\dagger (\partial_\mu \Phi + A_\mu \Phi) \rangle, \quad (4.2)$$

where the Goldstone field $\Phi = 2mU$ and U is a unitary matrix, which one can parametrize as $\exp \pi$, with π in the adjoint representation.

In order to minimize the amount of diagrams in a two-loop calculation, we follow a suggestion by Jackiw and Pi [41]. We aim at integrating out the Goldstone field: a gauge fixing is chosen which depends only on W_μ , and a change of variables is performed as

$$A_\mu \rightarrow U^{-1} A_\mu U - U^{-1} \partial_\mu U \equiv A_\mu^U, \quad (4.3)$$

which is just a gauge transformation thus leaving the gauge-invariant S_G and Δ unchanged. \mathcal{L}_σ becomes a mass term for the gauge field,

$$\mathcal{L}_\sigma = \frac{1}{2} m A_\mu^a A_\mu^a. \quad (4.4)$$

The definition of the Faddeev-Popov compensator directly leads to the following relation in dimensional regularization [42],

$$\int d\pi \Delta e^{-\frac{1}{2} S_{GF}(A^U)} = 1. \quad (4.5)$$

After all these steps we arrive at a simple massive Yang-Mills theory plus a one-loop subtraction term,

$$\mathcal{L} = \frac{1}{4} F_{\mu\nu}^a F_{\mu\nu}^a + \frac{1}{2} m^2 W_\mu^a W_\mu^a - \frac{l}{2} m^2 W_\mu^a W_\mu^a, \quad (4.6)$$

with

$$F_{\mu\nu}^a = \partial_\mu W_\nu^a - \partial_\nu W_\mu^a + \sqrt{l} g \epsilon^{abc} W_\mu^b W_\nu^c. \quad (4.7)$$

This is the model, which we first investigate in a two-loop calculation. For the gauge group we choose $SU(2)$, for the dimension $d = 3 - 2\epsilon$.

It has to be pointed out, that we integrate out the Goldstone and ghost fields exactly in an arbitrary gauge. In the resulting massive Yang-Mills theory one does not need any additional gauge

fixing terms. One can also view this massive Yang-Mills theory as a non-linear σ -model (with R_ξ -gauge fixing) in unitary gauge, i. e. in the limit $\xi \rightarrow \infty$. In section 2.2, it was already shown, that the on-shell one-loop self-energies coincide in the non-linear σ -model and in massive Yang-Mills theory, as to this order it is a gauge-invariant quantity.

4.2 Motivations for a two-loop calculation

We saw in chapter 2 that several authors have extracted a gap mass at one-loop level via gap equations. They all differ by the added and subtracted mass term in their model. The one loop results varied from $m_{SM} = 0.28 g^2$ in the non-linear σ -model to $m_{AN} = 0.38 g^2$ in Alexanian and Nair's calculation. Why is it now necessary to perform a two-loop calculation?

- The loop expansion does not correspond to an expansion in a small parameter $\frac{g^2}{m}$. Nevertheless, it might very well be that the one-loop results provide reasonable approximations of the true mass gap. This can only be tested by a two-loop calculation.
- If the whole method is consistent, the numerical values for the mass gap in the different models should converge at higher loop-orders, since to all orders they describe the same Yang-Mills theory. In this case one expects the two-loop correction to be of order $m_{AN} - m_{SM}$.
- The two-loop gap equation is quadratic in m , whereas at one loop it is linear. The existence of a positive solution is a non-trivial check of the whole approach.

The gap equation approach can only be a consistent method to calculate a magnetic mass, if the two-loop result fulfills all these requirements.

4.3 Two-loop self-energy in resummed massive Yang-Mills theory

Consider the Lagrangian of eq. (4.6) and (4.7) in $d = 3 - 2\epsilon$ dimensions and with the gauge group $SU(2)$. It is equivalent to a resummed non-linear σ -model in unitary gauge. The advantage of this gauge is that only a minimal amount of diagrams has to be calculated. The gap equation (2.4) has to be expanded up to $O(l^2)$, which requires the evaluation of the diagrams depicted in figure 4.1. The contribution of the one-loop diagrams to the transverse self-energy were already calculated in section 2.3.

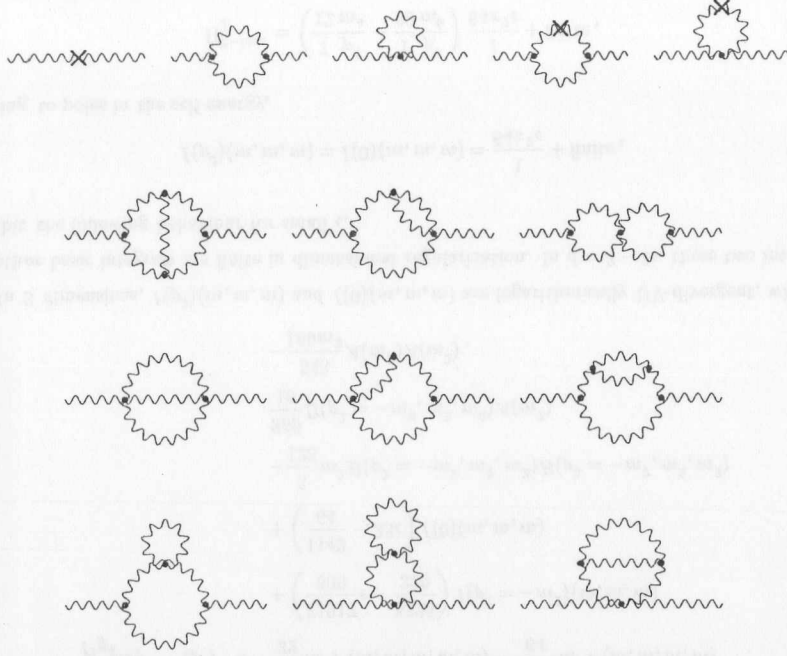


Figure 4.1: Diagrams contributing to the two-loop gap equation in the unitary gauge

Let us first concentrate on the one-loop counter-term diagrams, which on mass-shell yield a contribution of $O(l^2 g^2 m)$ to the self-energy. The calculation is fairly straightforward. With the help of the recurrence relation

$$\int \frac{d^3 k}{(2\pi)^3} \frac{1}{(k^2 + m^2)^2 ((k+p)^2 + m^2)} = -\frac{1}{2m^2(p^2 + 4m^2)} A_0(m^2), \quad (4.8)$$

one can write the result for diagrams 4 and 5 as a linear combination of A_0 and B_0 . The transverse part of the sum of diagrams 4 and 5 is

$$\frac{1}{l^2 g^2} \Pi_T^{1-loop-CT}(p^2) = \left(4m^2 + \frac{p^4}{m^2} - \frac{1}{4} \frac{p^6}{m^4} \right) B_0(p^2, m^2, m^2)$$

$$+ \left(2 - 2 \frac{p^2}{m^2} + \frac{1}{2} \frac{p^4}{m^4} \right) A_0(m^2), \quad (4.9)$$

which on-shell becomes

$$\Pi_T^{1-loop-CT}(p^2 = -m^2) = \frac{1}{8\pi} \left(\frac{21}{4} \ln 3 - 9 \right) l^2 g^2 m. \quad (4.10)$$

In order to evaluate the pole of the vector boson propagator, we also need the derivative of the one-loop self-energy (see eq. (2.4)), $\frac{\partial}{\partial p^2} \Pi_T^{1-loop}$, which contributes to $O(l^2 \frac{g^2}{m})$. The off-shell self-energy in unitary gauge is calculated in [35], leading directly to

$$\frac{\partial}{\partial p^2} \Pi_T^{1-loop}(p^2 = -m^2) = \frac{1}{32\pi} \left(33 - \frac{21}{4} \ln 3 \right) l \frac{g^2}{m}. \quad (4.11)$$

Far more work has to be done for the evaluation of the remaining 9 generic two-loop diagrams, which contribute to $O(l^2 g^4)$ to the gap equation.

Using the transverse projector,

$$P_T^{\mu\nu} = \frac{1}{2} (1 + \epsilon) \left(\delta_{\mu\nu} - \frac{p_\mu p_\nu}{p^2} \right), \quad (4.12)$$

the reduction program in FORM yields for the sum of the transverse parts

$$\begin{aligned} \frac{1}{l^2 g^4} \Pi_T^{2-loop}(p^2) = & \left(\frac{63}{4} m^4 - \frac{111}{8} p^2 m^2 - \frac{67}{16} p^4 - \frac{33}{32} \frac{p^6}{m^2} + \frac{1}{16} \frac{p^8}{m^4} \right) F(m, m, m, m, m) \\ & + \left(-\frac{63}{2} m^2 - \frac{113}{8} p^2 - \frac{27}{16} \frac{p^4}{m^2} + \frac{109}{64} \frac{p^6}{m^4} \right) V(m, m, m, m) \\ & + \left(-\frac{189}{2} \frac{m^4}{p^2} + \frac{237}{4} m^2 + \frac{12257}{80} p^2 - \frac{21}{8} \frac{p^4}{m^2} - \frac{167}{80} \frac{p^6}{m^4} \right) I_{211}(m, m, m) \\ & + \left(\frac{63}{4} \frac{m^2}{p^2} - \frac{111}{8} - \frac{159}{16} \frac{p^2}{m^2} + \frac{463}{192} \frac{p^4}{m^4} - \frac{1}{60} \frac{p^6}{m^6} \right. \\ & \left. - \frac{387}{4} \frac{m^2}{p^2} \epsilon + \frac{903}{8} \epsilon + \frac{1597}{20} \frac{p^2}{m^2} \epsilon - \frac{149}{15} \frac{p^4}{m^4} \epsilon - \frac{1}{50} \frac{p^6}{m^6} \epsilon \right) I_{111}(p^2)(m, m, m) \\ & + \left(-\frac{63}{4} \frac{m^2}{p^2} + \frac{111}{8} + \frac{159}{16} \frac{p^2}{m^2} - \frac{117}{64} \frac{p^4}{m^4} \right. \\ & \left. + \frac{135}{4} \frac{m^2}{p^2} \epsilon - \frac{195}{8} \epsilon - \frac{207}{8} \frac{p^2}{m^2} \epsilon - \frac{3}{4} \frac{p^4}{m^4} \epsilon \right) I_{111}(0)(m, m, m) \\ & + \left(\frac{37}{4} m^2 - \frac{5}{2} p^2 - \frac{387}{32} \frac{p^4}{m^2} - \frac{1}{32} \frac{p^6}{m^4} + \frac{35}{128} \frac{p^8}{m^6} - \frac{1}{64} \frac{p^{10}}{m^8} \right) B(p^2, m^2, m^2) B(p^2, m^2, m^2) \end{aligned}$$

$$\begin{aligned}
& + \left(\frac{23}{2} - \frac{151}{8} \frac{p^2}{m^2} - \frac{57}{8} \frac{p^4}{m^4} + \frac{1}{4} \frac{p^6}{m^6} + \frac{1}{16} \frac{p^8}{m^8} \right) B(p^2, m^2, m^2) A(m^2) \\
& + \left(-\frac{25}{8} \frac{1}{m^2} + \frac{7}{8} \frac{p^2}{m^4} + \frac{87}{160} \frac{p^4}{m^6} - \frac{1}{16} \frac{p^6}{m^8} \right) A(m^2) A(m^2). \quad (4.13)
\end{aligned}$$

If one expands the basic integrals of appendix C around $p^2 = 0$ and takes $\epsilon \rightarrow 0$, the terms $\sim \frac{1}{p^2}$ in eq. (4.13) cancel, leaving a well-defined limit $p^2 \rightarrow 0$ as required. The sum of the longitudinal parts turns out to be 0 for all external momenta p ,

$$\Pi_L^{2-loop}(p^2) = 0, \quad (4.14)$$

which is a nice check of the calculation. Setting $p^2 = -m^2$ in eq. (4.13) one obtains ¹

$$\begin{aligned}
\frac{1}{l^2 g^4} \Pi_T^{2-loop}(p^2) &= \frac{849}{32} m^4 F(m, m, m, m, m) - \frac{1329}{64} m^2 V(m, m, m, m) \\
&+ \left(\frac{71917}{600} \epsilon - \frac{5523}{320} \right) I(p^2 = -m^2)(m, m, m) \\
&+ \left(\frac{1143}{64} - 33\epsilon \right) I(0)(m, m, m) \\
&- \frac{3}{128} m^2 B(p^2 = -m^2, m^2, m^2) B(p^2 = -m^2, m^2, m^2) \\
&\frac{369}{16} B(p^2 = -m^2, m^2, m^2) A(m^2) \\
&- \frac{543}{160 m^2} A(m^2) A(m^2), \quad (4.15)
\end{aligned}$$

In 3 dimensions, $I(p^2)(m, m, m)$ and $I(0)(m, m, m)$ are logarithmically UV-divergent, whereas all other basic integrals are finite in dimensional regularization. In $d = 3 - 2\epsilon$, these two integrals exhibit the following behaviour for small ϵ ,

$$I(p^2)(m, m, m) = I(0)(m, m, m) = \frac{1}{64\pi^2\epsilon} + \text{finite}, \quad (4.16)$$

leading to poles in the self-energy,

$$\Pi_T^{2-loop} = \left(\frac{7}{12} \frac{p^4}{m^4} - \frac{1}{60} \frac{p^6}{m^6} \right) \frac{1}{64\pi^2\epsilon} + \text{finite}, \quad (4.17)$$

¹The on-shell two-loop self-energy for an arbitrary dimension d is written in appendix B. The result of the reduction of the 9 generic two-loop diagrams was also obtained using a FORM package written independently by O. Tarasov.

which cannot be dealt with by a mass or wave function renormalization. As we will see in the next section, this due to the bad high-energy behaviour of the propagator in unitary gauge. A similar problem arises already at one loop in cutoff-regularization, which was discussed in section 2.4. Calculations of counter-terms cannot be done in unitary gauge. However, if one is interested in finite parts of gauge-invariant quantities like poles in propagators, it provides a convenient short-cut of the calculation.

Let us now look at the corresponding calculation in Feynman gauge of a resummed non-linear σ -model.

4.4 Two-loop calculation in renormalizable gauges

In this section, we calculate the two-loop self-energy for the vector field in the resummed non-linear σ -model introduced in section 2.3 using a finite gauge parameter ξ . In this case, many more diagrams have to be evaluated, as ghost and Goldstone bosons are not integrated out. The diagrams are depicted in figures 4.2, 4.3.

First let us look at the one-loop counter-term diagrams with an arbitrary gauge parameter ξ . Its on-shell value, which contributes to the gap equation, reads

$$\Pi_T^{1-loop}(p^2 = -m^2) = \frac{1}{8\pi} \left(\frac{21}{4} \ln 3 - 9 + \frac{1}{4\sqrt{\xi}} \ln 3 + \sqrt{\xi} (3 - \ln 3) \right) l^2 g^2 m. \quad (4.18)$$

This quantity is not gauge-parameter independent. The resummation counter-terms, i.e. the mass counter-terms for the vector, ghost and Goldstone field, destroy BRS-invariance. In eq. (2.23), only \mathcal{L}_R exhibits a BRS-invariance, leading to a gauge-invariant pole of the propagator in every order in perturbation theory, if we neglect \mathcal{L}_1 . If one includes the terms of \mathcal{L}_1 , one loses gauge-parameter independence in the two-loop gap equation. To one loop, the gap mass is gauge-invariant, since the only contribution from \mathcal{L}_1 arises from a tree-graph contributing lm^2 to the gap equation. The ξ dependence is clearly a deficit of the resummation method we used. To all orders in perturbation theory, the ξ -dependence has to vanish. In our case, the calculation is only meaningful, if the numerical dependence of the two-loop gap mass on the gauge parameter is small.

The derivative of the one-loop self-energy is also gauge-parameter dependent,

$$\frac{\partial}{\partial p^2} \Pi_T^{1-loop}(p^2 = -m^2) = \frac{1}{8\pi} \left(\frac{33}{4} - \frac{21}{16} \ln 3 + \left(\xi - \frac{1}{4} \right) \ln \frac{2\sqrt{\xi} + 1}{2\sqrt{\xi} - 1} - 3\sqrt{\xi} \right) l \frac{g^2}{m}, \quad \xi > \frac{1}{4}. \quad (4.19)$$

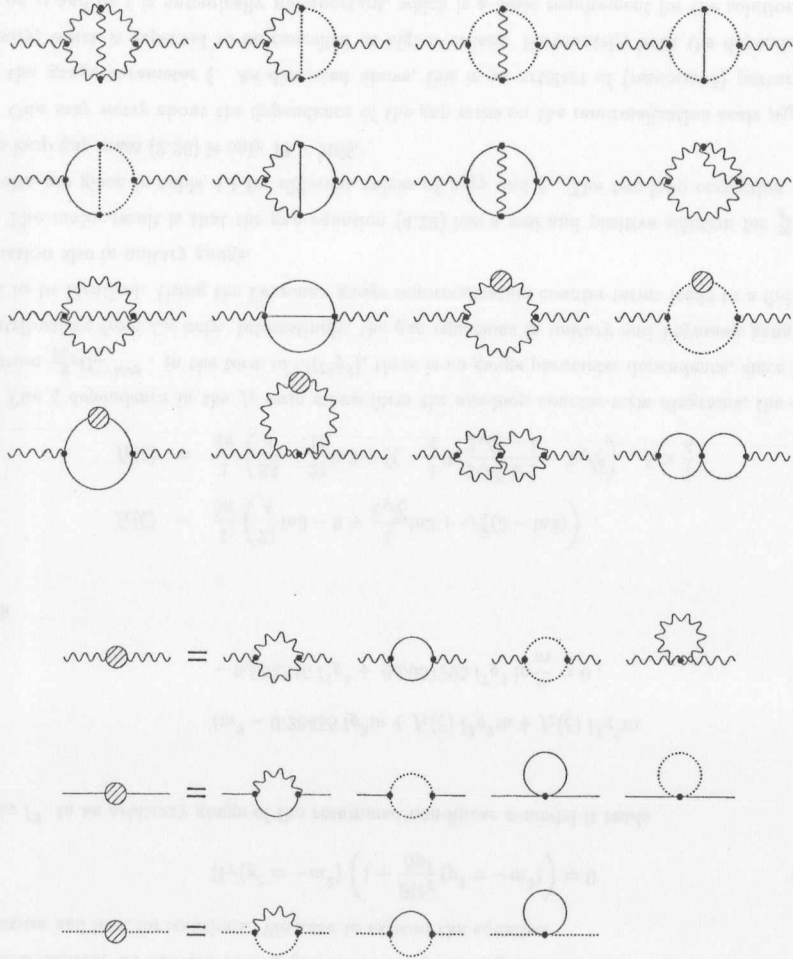


Figure 4.2: Generic two-loop self-energy diagrams in the non-linear σ -model

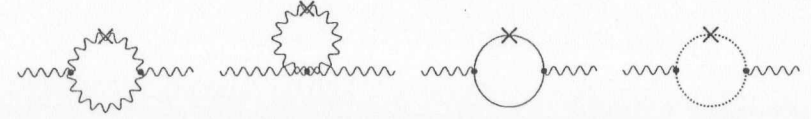


Figure 4.3: One-loop counter-term diagrams in the non-linear σ -model

In the sum of the transverse parts of the generic two-loop diagrams Π_T^{2-loop} , the coefficients of products of one-loop basic integrals contain ξ -dependent terms which do not cancel on mass-shell. However, this dependence combined with the ξ -dependence in $\frac{\partial}{\partial p^2} \Pi_T^{1-loop}$ leads to a gauge-invariant result for $\Pi_T(p^2 = -m^2) \left(1 + \frac{\partial}{\partial p^2} \Pi_T(p^2 = -m^2)\right)$ at the two-loop level, if one neglects the resummation counter-terms. This quantity is nothing but the two-loop pole of the propagator, which should be gauge-invariant in BRS-symmetric theories.

In order to check the preceding statements, the generic two-loop diagrams of the non-linear σ -model in Feynman gauge, $\xi = 1$, are calculated in appendix B. Neglecting counter-terms from resummation, we obtain the same position for the pole of the propagator as in unitary gauge. This constitutes a very stringent test for the algorithm we use.

The Feynman gauge is a renormalizable gauge. Collecting the coefficients of $I(p^2)(m, m, m)$ and $I(0)(m, m, m)$, we get the following poles in ϵ for the self-energy

$$\frac{1}{l^2 g^4} \Pi_{T, \xi=1}^{2-loop}(p^2) = \left(\frac{7}{12} - \frac{1}{60} \frac{p^2}{m^2} \right) \frac{1}{64\pi^2 \epsilon} + \text{finite} . \quad (4.20)$$

In order to get a finite result for the gap mass, we have to add counter-terms, which are $\sim l^2$ to the Lagrangian. To one loop the self-energy is finite in 3 dimensions in dimensional regularization, a already shown in chapter 2. According to eq. (4.20), to two-loop order a mass and wave function renormalization removes the infinities in the self-energy. This is also suggested by naive power counting.

We use the \overline{MS} -scheme here. Renormalization in Feynman gauge introduces a renormalization scale $\mu_{\overline{MS}}$ into the gap equation. This imposes another requirement on the solution of the gap equation: its numerical dependence on $\mu_{\overline{MS}}$ should be small.

4.5 Two-loop gap equation in the non-linear σ -model

In this section, we use the results gained in the preceding sections to set up the two-loop gap equation and look for solutions. We have to expand the equation

$$\Pi_T(p^2 = -m^2) \left(1 + \frac{\partial \Pi_T}{\partial p^2}(p^2 = -m^2) \right) = 0 \quad (4.21)$$

up to l^2 . In an arbitrary gauge of the resummed non-linear σ -model it reads

$$lm^2 - 0.28455 l^2 g^2 m + f_1(\xi) l^2 g^2 m + f_2(\xi) l^2 g^2 m - 0.064346 l^2 g^4 + 0.0037995 l^2 g^4 \ln \frac{\mu}{m} = 0, \quad (4.22)$$

with

$$f_1(\xi) = \frac{1}{8\pi} \left(\frac{21}{4} \ln 3 - 9 + \frac{1}{4\sqrt{\xi}} \ln 3 + \sqrt{\xi} (3 - \ln 3) \right),$$

$$f_2(\xi) = \frac{1}{8\pi} \left(\frac{33}{4} - \frac{21}{16} \ln 3 + \left(\xi - \frac{1}{4} \right) \ln \frac{2\sqrt{\xi} + 1}{2\sqrt{\xi} - 1} - 3\sqrt{\xi} \right), \quad \xi > \frac{1}{4}. \quad (4.23)$$

The ξ dependence in the f_1 -term stems from the one-loop counter-term diagrams, the one in f_2 from $\frac{\partial}{\partial p^2} \Pi_T^{1-loop}$. In the term of $O(l^2 g^4)$, there is no gauge parameter dependence, since it gets contributions from \mathcal{L}_R only. Interestingly, the gap equations in unitary and Feynman gauge turn out to be identical. Using the Feynman gauge renormalization counter-terms leads to a finite gap equation also in unitary gauge.

The major result is that the gap equation (4.22) has a real and positive solution for $\frac{m}{g^2}$. The results are given in table 4.1 for different values of $\mu_{\overline{MS}}$ and ξ . The two-loop correction to the one-loop gap mass (2.26) is only 15 – 20%.

One may worry about the dependence of the gap mass on the renormalization scale $\mu_{\overline{MS}}$ and on the gauge parameter ξ . As discussed above, this is an artefact of (resummed) perturbation theory, which is expected to be cancelled at higher orders. Fortunately, both the dependence of $\frac{m}{g^2}$ on μ and on ξ is numerically unimportant, which is a basic requirement for the solution to be meaningful. It suggests that the solution constitutes a reliable approximation to the exact gluon propagator mass in $SU(2)$ gauge theory.

The two-loop result survives all the crucial tests which have been mentioned in section 4.2 unexpectedly well: the quadratic gap equation has a real and positive solution, which is not far

$\frac{\mu}{m}$	0.3	1	3
$\frac{m}{g^2}, \xi = 1, \infty$	0.343	0.335	0.327
$\frac{m}{g^2}, \xi = 2$	0.345	0.336	0.328
$\frac{m}{g^2}, \xi = 10$	0.350	0.342	0.334

Table 4.1: Solutions of the two-loop gap equation

away from the one-loop result. Moreover, it is now in better agreement with Alexanian and Nair's gap mass and, above all, matches perfectly the lattice result obtained by Karsch et. al.

There is still one weak point in the present calculation: the non-renormalizability of the non-linear σ -model. To judge the significance of the result in the non-linear case, it is crucial to perform the whole calculation in the linear Higgs model, which is super-renormalizable. This will be done in the next chapter.

Chapter 5

Two-loop Gap Equation in the $SU(2)$ Higgs Model

In this chapter, we investigate two-loop effects on the gap equation in the 3-dimensional Higgs model. It is shown that the non-linear σ -model constitutes a reliable approximation for infrared phenomena in the Higgs model, and thereby also for the electroweak Standard model.

5.1 One-loop gap equations revisited: Landau versus Feynman gauge

In the non-linear σ -model, the one-loop gap equation is independent of the gauge parameter. In the linear model, one has to solve the coupled set of three equations (2.16) with three unknown variables, v , m and M , varying λ and μ^2 as parameters. The requirement of the third equation, that the vacuum expectation value of the Higgs field remains at zero, is manifestly gauge parameter dependent, since v is not a physical observable. This results in a gauge parameter dependent gap mass. The weak gauge dependence has to be cancelled at higher orders, since the gap mass should be a gauge-invariant quantity.

In the two-loop calculation, we will not solve the complete set of three two-loop gap equation, but restrict ourselves to the first of eqs. (2.16), the gap equation for the vector boson mass. For different values of $z = M/m$, we insert the corresponding μ and v from the one-loop solution and then solve the equation for m . We also investigate the dependence of m on varying μ and v around the one-loop value.

The two-loop gap equation for the vector boson is gauge parameter dependent. First, as in the

z	1	1.2	1.4	1.6	1.8
$\frac{\mu^2}{g^4}$	0.132	0.180	0.242	0.322	0.426
$\frac{v}{g}$	0.178	0.178	0.173	0.166	0.157
$\frac{m}{g^2}$	0.285	0.290	0.292	0.294	0.295

Table 5.1: Solutions of the one-loop gap equation in Landau gauge

z	1	1.2	1.4	1.6	1.8
$\frac{\mu^2}{g^4}$	0.111	0.153	0.208	0.277	0.367
$\frac{v}{g}$	0.159	0.162	0.160	0.155	0.148
$\frac{m}{g^2}$	0.226	0.231	0.234	0.236	0.237

Table 5.2: Solutions of the one-loop gap equation in Feynman gauge

one-loop case caused by a ξ -dependent v . Second, as in the two-loop case in the non-linear σ -model due to the one-loop (resummation) counterterm diagrams. The two-loop calculation in the linear Higgs model is performed in Feynman gauge, in contrast to the one-loop calculation in [28], where Landau gauge, $\xi = 0$, is used. For a suitable comparison of one- and two-loop results, we first solve the one-loop gap equations in Feynman gauge.

In table 5.1 and 5.2, we calculate the one-loop solutions for μ , v and m for different values of z , with $\frac{\lambda}{g^2} = \frac{1}{8}$. We use Landau, $\xi = 0$, and Feynman gauge, $\xi = 1$. The equations are listed in [28]. From the treatment in Landau gauge in [28] we see, that $1 \leq z \leq 2$ is a reasonable choice for the symmetric phase. $z \geq 2$ is forbidden, since in this case the Higgs boson can decay into two vector bosons. As a consequence of this, there will be poles in the two-loop result for the self-energy for $M = 2m$. The one-loop gap equation for M is complex for $z > 2$.

It can be seen that in both gauges there is a constant value for the vector boson mass deeply in the symmetric phase. There is, however, an obvious difference (20%) in the numerical value.

5.2 Two-loop self-energy for the Higgs field

The generic two-loop Higgs self-energy diagrams are depicted in figures 5.1 and 5.2. The sum of these diagrams is evaluated on mass-shell, $p^2 = -M^2$. The lengthy expressions resulting from the reduction to basic integrals can be found in appendix D in Feynman and in unitary gauge. The unitary gauge result differs from the result in Feynman gauge only by products of one-loop integrals. Quantitatively,

$$\begin{aligned} & \Sigma_{\xi=1}^{2-loop}(p^2 = -M^2) - \Sigma_{\xi=\infty}^{2-loop}(p^2 = -M^2) = \\ & \Sigma_{\xi=1,\infty}^{1-loop}(p^2 = -M^2) \left(\frac{\partial}{\partial p^2} \Sigma_{\xi=1}^{1-loop}(p^2 = -M^2) - \frac{\partial}{\partial p^2} \Sigma_{\xi=\infty}^{1-loop}(p^2 = -M^2) \right). \end{aligned} \quad (5.1)$$

This ensures that neglecting the resummation counter-terms, the pole of the Higgs boson propagator is gauge parameter independent to two loops. The underlying reason for this powerful check of the calculation is the BRS-invariance of the linear model. Eq. (5.1) can be verified using the expressions in appendix D and the one-loop results in [28] and section 2.2.

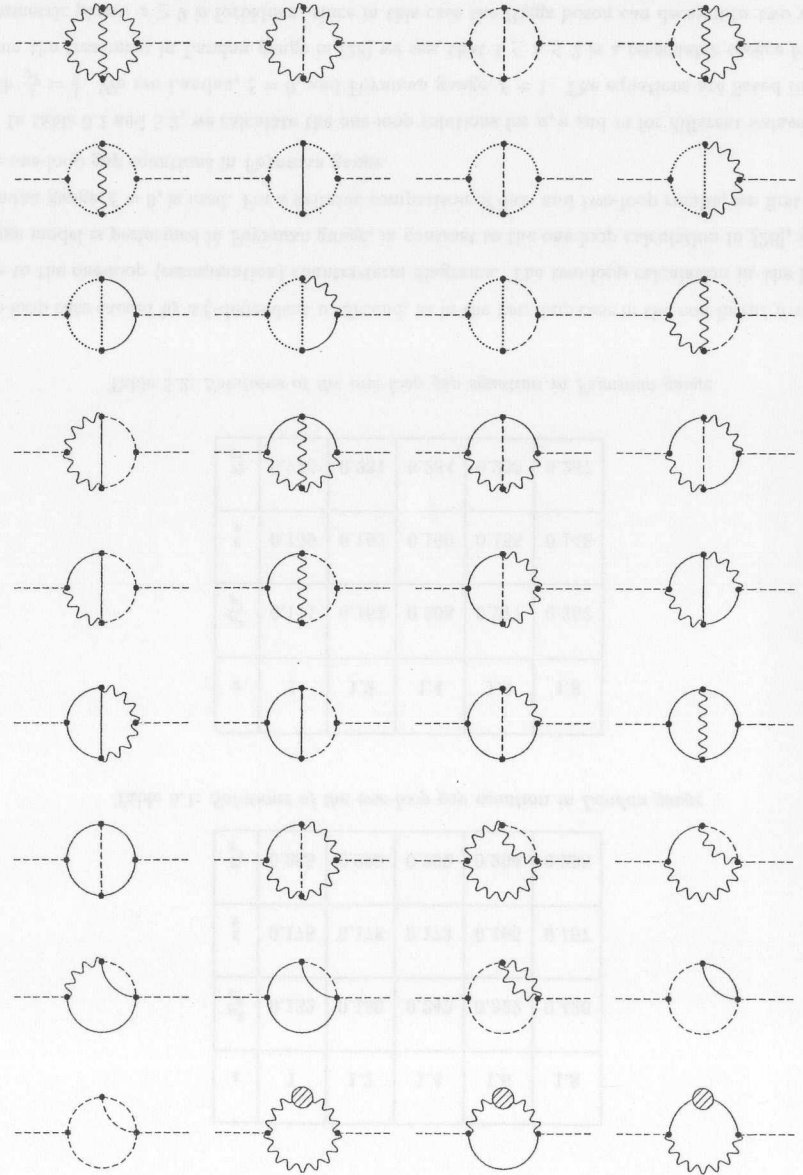
Concerning renormalization, eq. (D.1) leads to the following pole structure in ϵ for the Higgs self-energy (keeping the external momentum p^2 arbitrary),

$$\Sigma^{2-loop}(p^2) = \left(\frac{51}{8} + \frac{9M^2}{4m^2} - \frac{3M^4}{8m^4} \right) \frac{1}{64\pi^2\epsilon} + \text{finite}. \quad (5.2)$$

As expected and already mentioned in chapter 1.2, there is no wave function renormalization necessary in the 3-dimensional linear Higgs model. We have to add only a mass renormalization counter-term for the Higgs field.

5.3 Two-loop self-energy for the vector field

The analogous calculation is performed for the vector boson field. The sum of the generic two-loop diagrams shown in figures 5.2 and 5.3 is evaluated in Feynman and unitary gauge in $d = 3 - 2\epsilon$ on mass-shell, $p^2 = -m^2$ (note, that we only draw those Feynman diagrams, whose transverse part is non-zero). The results are written in appendix D.



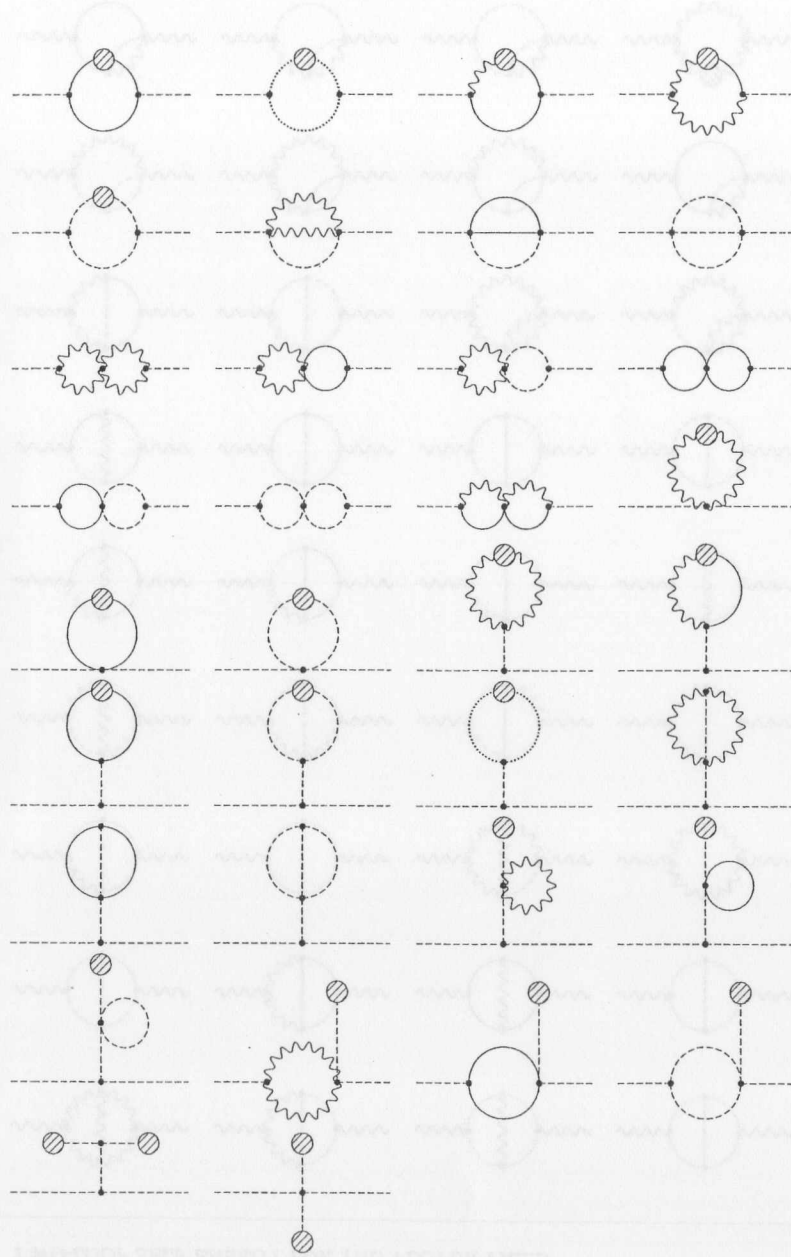


Figure 5.1: Two-loop diagrams for the Higgs self-energy

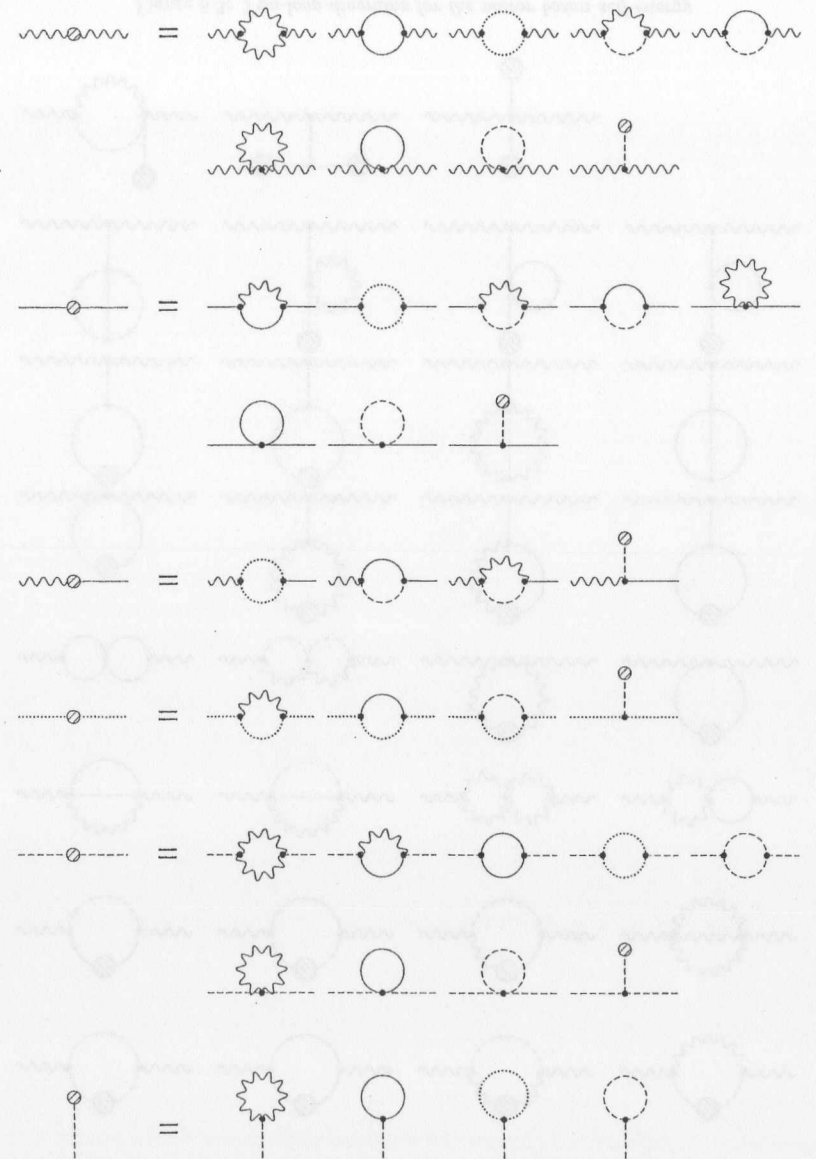


Figure 5.2: One-loop self-energy insertions into two-loop diagrams

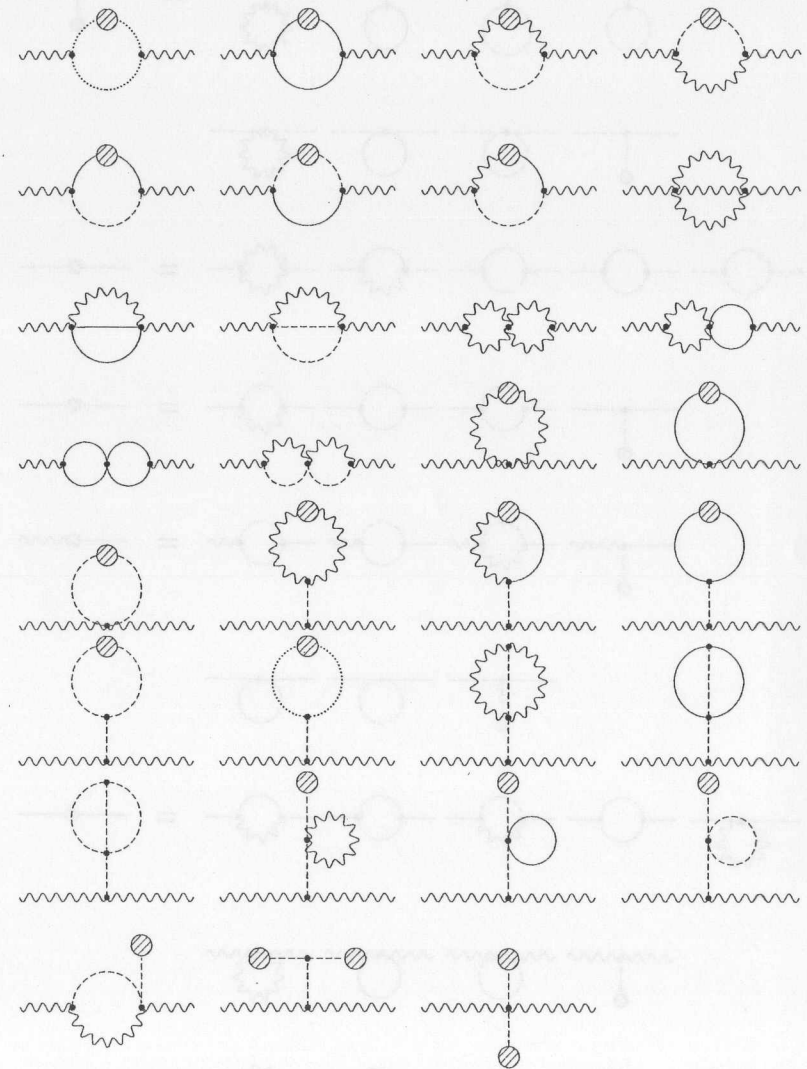
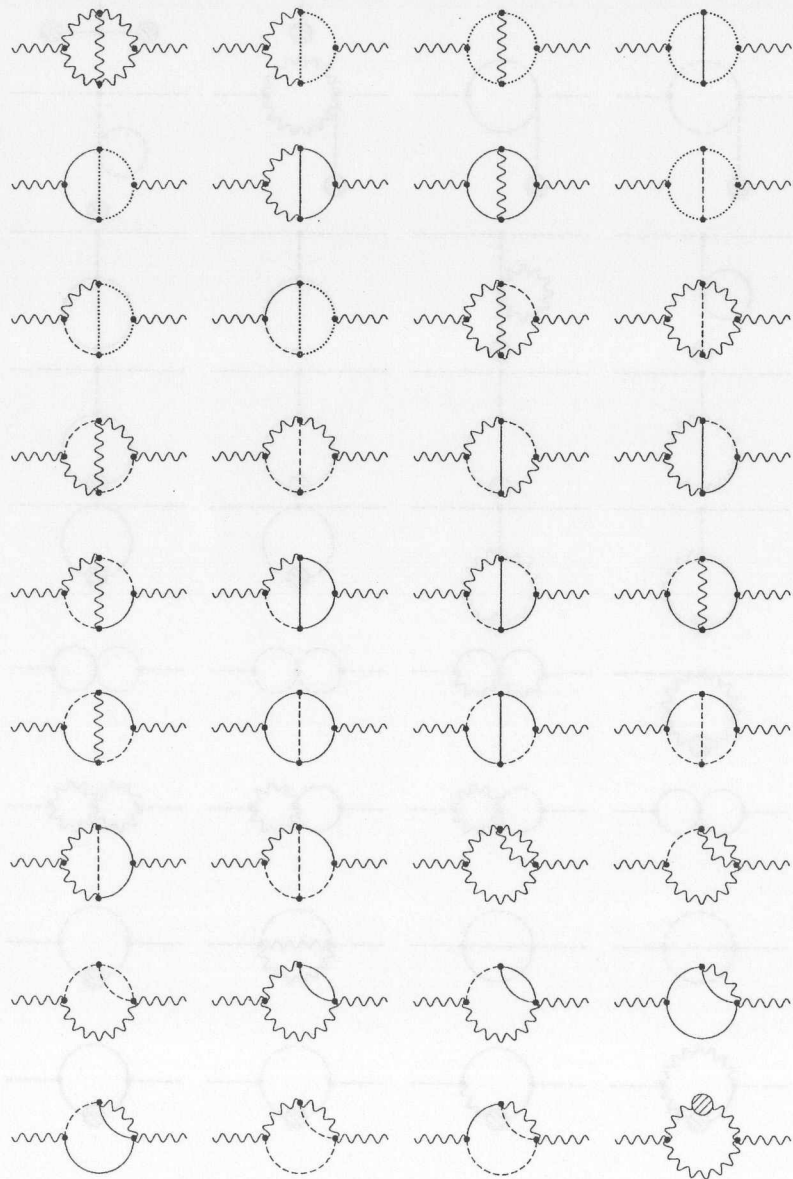


Figure 5.3: Two-loop diagrams for the vector boson self-energy

A relation similar to eq. (5.1) holds for the transverse two-loop vector field self-energy. It can be shown, that the pole of the transverse part of the vector boson propagator is gauge-invariant. In dimensional regularization, the divergent terms in the vector self-energy (evaluated for arbitrary external momentum p^2) can be obtained from eq. (D.2),

$$\Pi_T^{2-loop}(p^2) = \left(\frac{51}{8} \frac{m^2}{M^2} + \frac{9}{4} - \frac{3}{8} \frac{M^2}{m^2} \right) \frac{1}{64\pi^2\epsilon} + \text{finite}. \quad (5.3)$$

As for the Higgs field, no wave function renormalization is needed for the vector field. There is only a renormalization of the vacuum expectation value. Comparing eq. (5.3) with eq. (5.2), one can see a simple relation between the divergent terms: the coefficient in front of $\frac{1}{\epsilon}$ in eq. (5.3) is just $\frac{m^2}{M^2}$ times the mass renormalization counter-term for the Higgs field (Ward-identity).

The proved gauge-invariance of the poles of the Higgs and vector boson propagator to two-loops (neglecting resummation counter-terms) constitutes a powerful test for our FORM package.

5.4 Two-loop gap equation for the vector boson

In this section, we aim at a calculation of the vector boson mass in the symmetric phase of the 3-dimensional linear Higgs model. Since solving the complete set of three gap equations (2.16) would be unnecessarily complicated, we will use the following short-cut. As already mentioned in section 5.1, we look at the gap equation for the vector boson mass for different values of $z = \frac{M}{m}$, which are typical for the symmetric phase according to the one-loop calculations. For μ^2 and v we will insert the corresponding one-loop results from table 5.2. As already explained, the gap equation is gauge parameter dependent. We restrict the discussion to Feynman gauge.

In setting up the vector field gap equation we have to insert the third equation of (2.16), that the vacuum expectation value of the shifted field σ' equals 0 up to $O(l^2)$. Diagrammatically, this equation is written in fig. 5.4. The sum of tree-level counter-term, one-loop, one-loop counter-term and generic two-loop tadpole diagrams has to vanish.

This condition reduces the amount of one-loop counter-term and generic two-loop self-energy diagrams which contribute to the first equation of (2.16), since the relations in figure 5.5 hold. Therefore we can leave out all the two-loop diagrams involving tadpoles as well as the one-loop counter-term diagrams which contain the scalar one-point function. The remaining one-loop diagrams with resummation counter-terms contributing to the first equation of (2.16) are depicted in fig. 5.6. Their on-shell value is given by

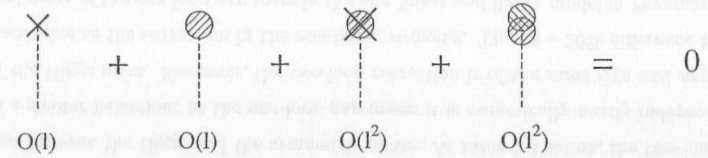


Figure 5.4: Two-loop gap equation for the Higgs-vev

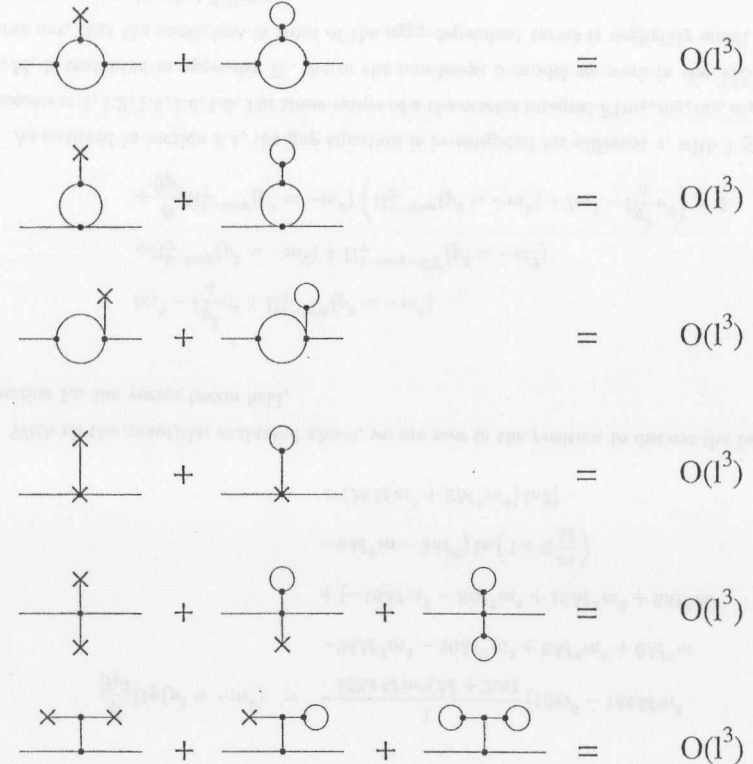


Figure 5.5: Cancellation of one-loop-CT and two-loop diagrams

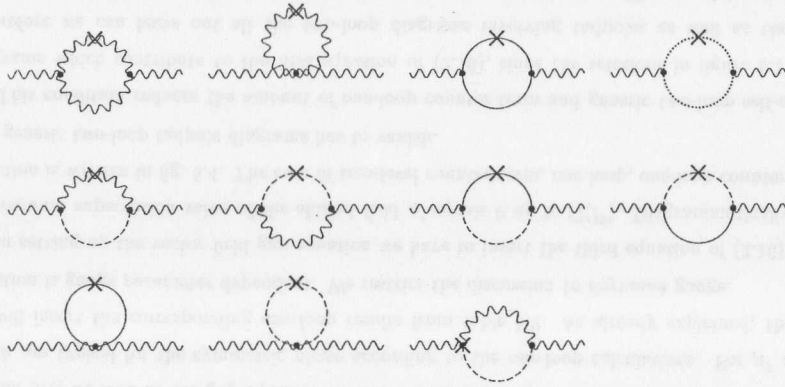


Figure 5.6: One-loop CT diagrams contributing to the gap equation

$$\begin{aligned}
\Pi_T^{1-loop-CT}(p^2 = -m^2) &= \delta m^2 \left[-\frac{1}{64\pi m} \left(50 + 2\frac{M}{m} + \frac{M^2}{m^2} \right) \right. \\
&+ \frac{1}{64\pi(2m+M)} \left(\frac{M^2}{m^2} + 8\frac{m^2}{M^2} - 4 \right) \\
&+ \frac{9}{16\pi m} \ln 3 + \frac{1}{32\pi} \frac{M^2}{m^3} \ln \left(1 + 2\frac{m}{M} \right) \left. \right] \\
&+ \delta M^2 \left[\frac{1}{64\pi} \left(3\frac{M}{m^2} - \frac{2}{m} - \frac{2}{M} \right) \right. \\
&+ \frac{1}{64\pi(2m+M)} \left(\frac{M^3}{m^3} - 4\frac{M}{m} + 8\frac{m}{M} \right) \\
&+ \frac{1}{32\pi m} \left(2 - \frac{M^2}{m^2} \right) \ln \left(1 + 2\frac{m}{M} \right) \left. \right] \\
&+ \frac{\delta V}{4\pi} \ln \left(1 + 2\frac{m}{M} \right) \\
&- (\mu^2 + \lambda v^2) \left[\frac{1}{64\pi m} \left(2 + 2\frac{M}{m} + \frac{M^2}{m^2} \right) \right. \\
&+ \frac{1}{64\pi(2m+M)} \left(4 - \frac{M^2}{m^2} \right) \\
&\left. - \frac{1}{32\pi} \frac{M^2}{m^3} \ln \left(1 + 2\frac{m}{M} \right) - \frac{1}{16\pi m} \ln 3 \right]. \quad (5.4)
\end{aligned}$$

We also need the derivative of the one-loop transverse self-energy on mass-shell. It reads

$$\begin{aligned}
\frac{\partial}{\partial p^2} \Pi_T(p^2 = -m^2) &= -\frac{1}{128\pi M m^4 (M+2m)} [16m^6 - 144Mm^5 \\
&- 96M^2m^4 - 20M^3m^3 + 6M^4m^2 + 6M^5m \\
&+ (-16Mm^5 - 8M^2m^4 + 16M^3m^3 + 8M^4m^2 \\
&- 6M^5m - 3M^6) \ln \left(1 + 2\frac{m}{M} \right) \\
&+ (18Mm^5 + 9M^2m^4) \ln 3]. \quad (5.5)
\end{aligned}$$

With all the quantities evaluated above, we are now in the position to discuss the two-loop gap equation for the vector boson field,

$$\begin{aligned}
lm^2 - l\frac{g^2}{4}v^2 + \Pi_T^{1-loop}(p^2 = -m^2) \\
+ \Pi_T^{2-loop}(p^2 = -m^2) + \Pi_T^{1-loop-CT}(p^2 = -m^2) \\
+ \frac{\partial}{\partial p^2} \Pi_T^{1-loop}(p^2 = -m^2) \left(\Pi_T^{1-loop}(p^2 = -m^2) + lm^2 - l\frac{g^2}{4}v^2 \right) = 0. \quad (5.6)
\end{aligned}$$

As outlined in section 5.1, the gap equation is investigated for different z , with $1 \leq z \leq 2$. We choose $z = 1, 1.2, 1.4, 1.6, 1.8$. For these values of z the master integral $F(m_1, m_2, m_3, m_4, m_5)$, $m_i = m, M$, is evaluated in appendix E. As in the non-linear σ -model we work in the \overline{MS} -scheme. It turns out, that the coefficient in front of the $\mu_{\overline{MS}}$ -dependent terms is negligibly small. Therefore, we set $\mu_{\overline{MS}} = m$ in what follows.

The solutions of eq. (5.6) for different values of z are listed in table 5.3. They are compared with the one-loop result in Feynman gauge.

For the scalar coupling $\frac{\lambda}{g^2}$, we choose $\frac{1}{8}$. For this value, a crossover behaviour was found for the transition between the Higgs and the symmetric phase. As table 5.3 shows, the two-loop solutions exhibits a similar behaviour as the one-loop gap mass: it is numerically nearly independent of the value of the Higgs mass. Moreover, the two-loop correction is of the same sign and approximately of the same size as the correction in the non-linear σ -model. The 15 – 20% difference between the numerical value of the one-loop gap mass in the non-linear and linear model in Feynman gauge still remains at two loops.¹

¹In the linear Higgs model, the dependence of the two-loop gap mass on the gauge parameter is not investigated

z	1	1.2	1.4	1.6	1.8
$\frac{m}{g^2}$ (one-loop)	0.226	0.231	0.234	0.236	0.237
$\frac{m}{g^2}$ (two-loop)	0.303	0.307	0.310	0.309	0.299

Table 5.3: Solutions of the two-loop gap equation in Feynman gauge

$z = 1.6, \frac{\mu^2}{g^4} = 0.277, \frac{v}{g} =$	0.1	0.155	2
$\frac{m}{g^2}$	0.303	0.309	0.317

Table 5.4: Solutions of the two-loop gap equation for different $\frac{v}{g}$

$z = 1.6, \frac{v}{g} = 0.155, \frac{\mu^2}{g^4} =$	0.177	0.277	0.377
$\frac{m}{g^2}$	0.304	0.309	0.315

Table 5.5: Solutions of the two-loop gap equation for different $\frac{\mu^2}{g^4}$

In solving eq. (5.6), the one-loop values for μ^2 and v are inserted for each value of z according to table 5.2. At two loops these values change, if one solves the set of three gap equations exactly. To estimate this effect, we vary μ^2 and v around the one-loop solutions of table 5.2 for a fixed value of z ($z = 1.6$) and show that there is only a small numerical influence on the two-loop gap mass (see tables 5.4 and 5.5).

The small numerical difference between the gap mass in the linear and non-linear model as well as the independence of the gap mass of the Higgs mass M shows that the non-linear σ -model describes the infrared limit of the linear Higgs model and of the electroweak Standard model at finite temperature to a very good approximation.

here. The one-loop solution suggests that the numerical dependence is bigger than in the non-linear σ -model, where it is almost negligible.

Summary and Conclusions

We have investigated gap equations for the magnetic mass to two-loop order. In particular we have looked at the following 3-dimensional theories: a resummed massive Yang-Mills theory, a resummed non-linear σ -model in arbitrary gauge and a resummed $SU(2)$ Higgs model in unitary and Feynman gauge. The one-loop approaches have been summarized and some additional calculations have been performed, in particular the one-loop self-energies of the vector and Higgs field in the Higgs model in unitary gauge. The one-loop self-energy for the vector boson in the non-linear σ -model has been recalculated in cut-off regularisation. In dimensional regularization all one-loop self-energies are finite. In cut-off regularization, the calculation in renormalizable gauges shows, that a mass renormalization counter-term has to be introduced into the non-linear σ -model at one-loop. The result for the gap mass is identical in both schemes. In unitary gauge, calculating to one-loop order with a cut-off leads to divergences with high powers of the external momentum which cannot be removed by a renormalization of the mass or the wave-function. This is because the unitary gauge is a non-renormalizable gauge.

The two-loop calculation of the transverse vector self-energy in the non-linear σ -model shows a similar behaviour even in dimensional regularization. In renormalizable gauges, we need a mass and wave-function renormalization, whereas in unitary gauge we again get powers in the external momentum which cannot be dealt with by the usual redefinition of parameters. To three-loop order naive power counting suggests that these problems arise also in renormalizable gauges. This is due to the non-renormalizability of the non-linear σ -model. In the linear Higgs model, however, we have seen that at the two-loop level a mass renormalization is sufficient in Feynman gauge, as expected in a renormalizable theory in 3 dimensions. In unitary gauge of the linear model, however, the problematic situation remains.

The two-loop gap equation in resummed massive Yang-Mills theory and in a resummed non-linear σ -model shows a real and positive solution for the vector boson mass: $m \approx 0.34g^2$. This is clearly a non-trivial result. It is only $\sim 20\%$ larger than the one-loop result and in very good

agreement with the lattice simulations of the propagator mass in Landau gauge and with the results of other one-loop models. The gap equation still contains a weak gauge dependence and a logarithmic dependence on the renormalization scale. It has been shown that they are numerically unimportant. This suggests that the solution constitutes a reliable approximation to the exact gluon propagator mass in an $SU(2)$ gauge theory.

A vector boson mass $\sim 0.34g^2$ is not in contradiction with confinement. It is of the same size as the confinement scale given by the string tension which was calculated in [44]. The connection of such a propagator mass to the heavier glueball masses $\sim O(1)g^2$ [25,45] in a 3-dimensional $SU(2)$ gauge theory remains to be clarified. We published the calculation in the non-linear σ -model in [46].

To judge the significance of a calculation in the non-renormalizable non-linear sigma model, we have performed the same calculation in the linear Higgs model, which is super-renormalizable. The vector-boson and Higgs self-energy have been calculated on mass-shell in Feynman and unitary gauge and the corresponding gap equation for the vector boson mass has been solved varying the Higgs mass.

The result for the gap mass is almost independent of the Higgs mass in the symmetric phase. This proves that the non-linear σ -model is a very good approximation for infrared phenomena of the linear Higgs model. Moreover, the two-loop correction in the linear model is of similar size as in the non-linear model.

The result of the two-loop calculation in the considered 3-dimensional models is a very strong hint that the gap equation approach is a reasonable way to calculate the transverse propagator mass of the vector boson in the symmetric phase. It is a crucial test for the consistency of the whole method. The physical interpretation and the connection to the masses of bound states seen on the lattice is not yet clear. This should be clarified by further research.

Appendix A

One-loop Integrals

The formulae for one-loop two-point integrals in 3 Euclidean dimensions are summarized. They are discussed in dimensional as well as in cut-off regularization.

In dimensional regularisation all propagator type integrals can be reduced to two basic integrals A_0 and B_0 defined in eq. (2.21), using simple cancellation techniques between numerator and denominator in integrals of Feynman diagrams and taking advantage of translational invariance. Integration yields

$$A_0(m^2) = \int d^3k \frac{1}{k^2 + m^2} = -\frac{m}{4\pi} \quad (\text{A.1})$$

and

$$B_0(p^2, m_1^2, m_2^2) = \int d^3k \frac{1}{(k^2 + m_1^2)((k+p)^2 + m_2^2)} = \frac{1}{4\pi p} \arctan \frac{p}{m_1 + m_2} \quad (\text{A.2})$$

The only non-trivial reduction relation in dimensional regularisation, used for the calculations in this thesis, is

$$\int d^3k \frac{(kq)^2}{(k^2 + m^2)} = -\frac{1}{3} m^2 q^2 A_0(m^2). \quad (\text{A.3})$$

Both in dimensional and cut-off regularization,

$$\int d^3k \frac{kq}{(k^2 + m^2)} = 0. \quad (\text{A.4})$$

In cut-off regularization a relation corresponding to eq. (A.3) is

$$\int^\Lambda d^3k \frac{(kq)^2}{(k^2 + m^2)} = -\frac{1}{18\pi^2} q^2 (\Lambda^3 - 3m^2\Lambda) + \text{finite}. \quad (\text{A.5})$$

The finite parts in all relations are identical in both regularization schemes. In cut-off regularization, there are also two other independent non-trivial integrals,

$$\begin{aligned} \int^\Lambda d^3k \frac{kq}{((k+q)^2 + m^2)} &= -\frac{1}{3\pi^2} q^2 \Lambda + \text{finite} \\ \int^\Lambda d^3k \frac{(kq)^2}{((k+q)^2 + m^2)} &= \frac{1}{18\pi^2} q^2 (\Lambda^3 - 3m^2\Lambda) + \frac{7}{30\pi^2} q^4 \Lambda + \text{finite}. \end{aligned} \quad (\text{A.6})$$

In dimensional regularization these integrals can be related to the ones of eq. (A.4) and (A.5) using translational invariance.

Appendix B

Two-loop Results in the Non-linear σ -model

In chapter 4, the transverse two-loop vector boson self-energy is calculated in $d = 3 - 2\epsilon$ dimensions on as well as off mass-shell. Here the on-shell result of the reduction is given in an arbitrary dimension d . The basic integrals are defined in eq. (3.19).

$$\begin{aligned}
\frac{1}{l^2 g^4} \Pi_T^{2-loop}(p^2) = & \\
& \frac{3}{16} m^4 \frac{176d - 245}{d - 1} F(m, m, m, m, m) \\
& - \frac{3}{16} m^2 \frac{144d^3 - 712d^2 + 1241d - 760}{(d - 1)^2} V(m, m, m, m) \\
& - \frac{1}{48} \frac{10800d^4 - 70632d^3 + 165227d^2 - 166654d + 61752}{(d - 1)^2(3d - 4)} I(p^2 = -m^2)(m, m, m) \\
& - \frac{3}{16} \frac{(d - 2)(32d^3 - 312d^2 + 656d - 405)}{(d - 1)^2} I(0)(m, m, m) \\
& + \frac{3}{32} \frac{32d^2 - 148d + 155}{(d - 1)^2} B(p^2 = -m^2, m^2, m^2) B(p^2 = -m^2, m^2, m^2) \\
& - \frac{3}{4} \frac{16d^4 - 188d^3 + 668d^2 - 940d + 465}{(d - 1)^2} B(p^2 = -m^2, m^2, m^2) A(m^2) \\
& - \frac{1}{8m^2} \frac{(2d - 3)(24d^5 - 164d^4 + 452d^3 - 680d^2 + 597d - 242)}{(d - 1)^2(3d - 4)} A(m^2) A(m^2), \quad (B.1)
\end{aligned}$$

Switching back to $d = 3 - 2\epsilon$, we write down the result for the off-shell transverse two-loop

self-energy of the vector field in Feynman gauge. It is

$$\begin{aligned}
\frac{1}{l^2 g^4} \Pi_T^{2-loop}(p^2) = & \\
& \left(\frac{257}{16} m^4 - \frac{351}{32} p^2 m^2 - \frac{1}{2} p^4 \right) F(m, m, m, m, m) \\
& + \left(-\frac{259}{8} m^2 - \frac{1265}{64} p^2 - \frac{261}{32} \frac{p^4}{m^2} \right) V(m, m, m, m) \\
& + \left(\frac{8163}{20} m^8 - \frac{4607}{80} p^2 m^6 - \frac{12183}{20} p^4 m^4 - \frac{12243}{80} p^6 m^2 - \frac{77}{8} p^8 \right) \frac{I_{211}(m, m, m)}{m^2 p^2 (p^2 + 4m^2)} \\
& + \left(-\frac{279}{4} m^6 + \frac{1409}{48} p^2 m^4 + \frac{53279}{960} p^4 m^2 + \frac{3923}{480} p^6 \right. \\
& \left. + \frac{8717}{20} m^6 \epsilon - \frac{14647}{60} p^2 m^4 \epsilon - \frac{225067}{600} p^4 m^2 \epsilon - \frac{5473}{100} p^6 \epsilon \right) \frac{I_{111}(p^2)(m, m, m)}{m^2 p^2 (p^2 + 4m^2)} \\
& + \left(+\frac{279}{4} m^6 - \frac{507}{16} p^2 m^4 - \frac{3585}{64} p^4 m^2 - \frac{261}{32} p^6 \right. \\
& \left. - \frac{655}{4} m^6 \epsilon - \frac{51}{8} p^2 m^4 \epsilon + \frac{537}{8} p^4 m^2 \epsilon + \frac{35}{4} p^6 \epsilon \right) \frac{I_{111}(0)(m, m, m)}{m^2 p^2 (p^2 + 4m^2)} \\
& + \text{products of one-loop integrals.} \quad (B.2)
\end{aligned}$$

The coefficients in front of the generic basic two-loop integrals coincide in unitary and Feynman gauge on mass-shell, see eq. (4.15).

We also present the transverse part of the master two-loop self-energy diagram with the topology  in the unitary gauge calculation of the non-linear σ -model. It is the most difficult diagram to reduce due to the high powers of momenta in the numerator (unitary gauge propagator + vector boson vertices). The result can best be used for a check of some reader's reduction program. That is why we give it in detail here, i.e. off-shell and for any dimension d ,

$$\begin{aligned}
\Pi_T^{\text{master}} = & \\
& \frac{1}{16} (288 d m^8 - 360 m^8 - 336 p^2 d m^6 + 564 p^2 m^6 + 250 p^4 m^4 - 128 p^4 d m^4 \\
& - 32 p^6 d m^2 + 63 p^6 m^2 + 2 p^8) F(m, m, m, m, m) / ((-1 + d) m^4) - \frac{1}{8} (-864 d m^6 \\
& + 384 d^2 m^6 + 480 m^6 + 122 m^4 p^2 + 114 m^4 p^2 d - 104 m^4 p^2 d^2 + 350 p^4 d m^2 \\
& - 152 p^4 d^2 m^2 - 153 m^2 p^4 - 5 p^6 + 8 p^6 d) V(m, m, m, m) / ((-1 + d)^2 m^4) - \frac{1}{12}
\end{aligned}$$

$$\begin{aligned}
& (p^2 + 9m^2)(p^2 + m^2)(-606m^4 - 1734m^4d^2 + 576m^4d^3 + 1764dm^4 + 5064m^2p^2d^2 \\
& - 1440m^2p^2d^3 - 5646p^2dm^2 + 1956p^2m^2 + 105p^4d^2 - 187p^4d + 76p^4) \\
I_{211}(m, m, m) & /((-1+d)^2p^2m^4(-4+3d)(-2+3d) - \frac{1}{72}(-17784p^4d^4m^4 \\
& - 44712p^2d^4m^6 - 32p^8 - 158652dm^8 + 45684m^8 + 409518p^2dm^6 - 121080p^2m^6 \\
& - 82668p^4m^4 + 262728p^4dm^4 + 12696p^6dm^2 - 4152p^6m^2 - 484926p^2m^6d^2 \\
& - 12255p^6m^2d^2 + 243576p^2m^6d^3 + 202824m^8d^2 - 111888m^8d^3 + 108p^8d \\
& - 100p^8d^2 - 282900p^4m^4d^2 + 122655p^4m^4d^3 + 4452p^6m^2d^3 - 576p^6d^4m^2 \\
& + 22032d^4m^8 + 24p^8d^3)I_{111}(p^2)(m, m, m)/((-1+d)^2p^2m^6(-4+3d)(-2+3d) + \frac{3}{8} \\
& (-78m^4p^2 + 126m^4p^2d - 48m^4p^2d^2 - 108dm^6 + 48d^2m^6 + 60m^6 + 85p^4dm^2 \\
& - 40p^4d^2m^2 - 34m^2p^4 - p^6 + 2p^6d)I_{111}(0)(m, m, m)/((-1+d)^2p^2m^4) + \frac{1}{32}(\\
& - 1808dm^{10} + 576d^2m^{10} + 1424m^{10} + 1168p^2m^8 - 1648p^2m^8d + 576p^2m^8d^2 \\
& + 1036p^4dm^6 - 416p^4d^2m^6 - 624m^6p^4 + 248p^6dm^4 - 80p^6d^2m^4 - 160p^6m^4 \\
& - p^8m^2 + 8p^8m^2d + p^{10})B(p^2, m^2, m^2)^2 /((-1+d)^2m^8) - \frac{1}{8}(p^2 + 4m^2)(124m^6 \\
& - 176dm^6 + 64d^2m^6 - 104m^4p^2d^2 - 210m^4p^2 + 292m^4p^2d - 18m^2p^4 \\
& + 15p^4dm^2 + p^6)B(p^2, m^2, m^2)A(m^2)/((-1+d)^2m^8) + \frac{1}{24}(-1223p^4d^4m^2 \\
& - 720p^2d^6m^4 - 4884p^2d^4m^4 + 3180p^2d^5m^4 + 1194p^4d^3m^2 - 192m^6 - 4500d^2m^6 \\
& + 1392dm^6 - 600m^4p^2d^2 - 376p^4d^2m^2 + 24p^6d^2 - 54p^6d^3 + 408p^4d^5m^2 \\
& + 618m^6d^5 + 72m^6d^6 + 3024p^2d^3m^4 + 27p^6d^4 + 6042m^6d^3 - 3468d^4m^6)A(m^2)^2 \\
& /((-1+d)^2d^2m^8(-4+3d)(-2+3d)).
\end{aligned}$$

Appendix C

Basic Integrals in $d = 3 - 2\epsilon$

We give analytic results of the basic integrals defined in eq. (3.19). Some misprints in [40] are corrected in the following formulae.

Only $I(p^2)(m_1, m_2, m_3)$ and $I(0)(m_1, m_2, m_3)$ show poles in ϵ for $d = 3 - 2\epsilon$. $F, V, I_{211}, I_{121}, I_{112}$ are finite in 3 dimensions. We define

$$\begin{aligned}
I_{111}(p^2)(m_1, m_2, m_3) &= \mu^{4\epsilon} \int \int \frac{d^{3-2\epsilon}k_1}{(2\pi)^{3-2\epsilon}} \frac{d^{3-2\epsilon}k_2}{(2\pi)^{3-2\epsilon}} \frac{1}{(k_1^2 + m_1^2)((k_2 - p)^2 + m_2^2)} \\
&\quad \frac{1}{((k_1 - k_2)^2 + m_3^2)}, \\
I_{111}(0)(m_1, m_2, m_3) &= \mu^{4\epsilon} \int \int \frac{d^{3-2\epsilon}k_1}{(2\pi)^{3-2\epsilon}} \frac{d^{3-2\epsilon}k_2}{(2\pi)^{3-2\epsilon}} \frac{1}{(k_1^2 + m_1^2)(k_2^2 + m_2^2)} \\
&\quad \frac{1}{((k_1 - k_2)^2 + m_3^2)}. \tag{C.1}
\end{aligned}$$

Integration yields,

$$\begin{aligned}
I_{111}(p^2)(m_1, m_2, m_3) &= \frac{1}{(4\pi)^2} \left(\frac{1}{4\epsilon} + \frac{3}{2} - \frac{m_1 + m_2 + m_3}{p} \arctan \frac{p}{m_1 + m_2 + m_3} \right. \\
&\quad \left. + \frac{1}{2} \ln \frac{\mu^2 \overline{MS}}{(m_1 + m_2 + m_3)^2 + p^2} \right) \\
I_{111}(0)(m_1, m_2, m_3) &= \frac{1}{(4\pi)^2} \left(\frac{1}{4\epsilon} + \frac{1}{2} + \ln \frac{\mu^2 \overline{MS}}{m_1 + m_2 + m_3} \right), \tag{C.2}
\end{aligned}$$

where

$$\mu_{MS}^2 = e^{-\gamma} 4\pi \mu^2. \quad (C.3)$$

The analytic result for $V(m_1, m_2, m_3, m_4)$ reads,

$$\begin{aligned} V(m_1, m_2, m_3, m_4) = & \frac{1}{(4\pi)^2 4pm_3} \left\{ 2 \ln \frac{m_2 + m_3 + m_4}{m_2 - m_3 + m_4} \arctan \frac{p}{m_1 + m_3} \right. \\ & + i \left[\text{Li}_2 \left(-\frac{m_1 + m_3 - ip}{m_2 - m_3 + m_4} \right) - \text{Li}_2 \left(-\frac{m_1 - m_3 - ip}{m_2 + m_3 + m_4} \right) \right. \\ & \left. \left. + \text{Li}_2 \left(-\frac{m_1 - m_3 + ip}{m_2 + m_3 + m_4} \right) - \text{Li}_2 \left(-\frac{m_1 + m_3 + ip}{m_2 - m_3 + m_4} \right) \right] \right\}, \quad (C.4) \end{aligned}$$

where the dilogarithm function is,

$$\text{Li}_2(x) = -\int_0^x \frac{\ln(1-t)}{t} dt. \quad (C.5)$$

For $F(m_1, m_2, m_3, m_4, m_5)$, there remains a one-dimensional integrals which has to be evaluated numerically. If only two masses are different, F is evaluated in appendix E. The expression in the general mass case is,

$$\begin{aligned} F(m_1, m_3, m_5, m_2, m_4) = & -\frac{2}{\sqrt{|\mathcal{M}(p, m_1, m_3, m_5, m_2, m_4)|}} \\ & \int_{M_0}^{m_5} \frac{|\mathcal{M}_H(p, m_1, m_3, x, m_2, m_4)|}{\sqrt{|\mathcal{M}(p, m_1, m_3, x, m_2, m_4)|}} x dx, \quad (C.6) \end{aligned}$$

where M_0 is a zero of $|\mathcal{M}(p, m_1, m_3, x, m_2, m_4)| = 0$, and $|\mathcal{M}|$ is the determinant of \mathcal{M} .

$$\mathcal{M}(p, m_1, m_2, m_3, m_4, m_5) = \begin{pmatrix} 2m_3^2 & m_1^2 + m_3^2 - m_4^2 & m_2^2 + m_3^2 - m_5^2 \\ m_1^2 + m_3^2 - m_4^2 & 2m_1^2 & m_1^2 + m_2^2 + p^2 \\ m_2^2 + m_3^2 - m_5^2 & m_1^2 + m_2^2 + p^2 & 2m_2^2 \end{pmatrix} \quad (C.7)$$

and

$$\mathcal{M}(p, m_1, m_2, m_3, m_5, m_5) = \begin{pmatrix} H_1 & H_2 & H_3 \\ m_1^2 + m_3^2 - m_4^2 & 2m_1^2 & m_1^2 + m_2^2 + p^2 \\ m_2^2 + m_3^2 - m_5^2 & m_1^2 + m_2^2 + p^2 & 2m_2^2 \end{pmatrix}, \quad (C.8)$$

with

$$\begin{aligned} H_1(p, m_1, m_2, m_3, m_4, m_5) &= H_1^3 - H_1^4 + H_2^3 - H_2^5, \\ H_2(p, m_1, m_2, m_3, m_4, m_5) &= H_2^1 + H_3^1 - H_3^4, \\ H_3(p, m_1, m_2, m_3, m_4, m_5) &= H_3^2 - H_3^5 + H_1^2, \quad (C.9) \end{aligned}$$

where

$$\begin{aligned} H_1^3 &= H_X(m_1, m_2, m_4, m_5), H_1^4 = H_Y(m_1, m_3, m_5, m_2), \\ H_2^3 &= H_X(m_2, m_1, m_5, m_4), H_2^5 = H_Y(m_2, m_3, m_4, m_1), \\ H_2^1 &= H_Z(m_4, m_2, m_3, m_5), H_3^1 = H_Z(m_4, m_3, m_2, m_5), \\ H_3^4 &= H_Z(m_1, m_3, m_5, m_2), H_3^5 = H_Z(m_5, m_3, m_1, m_4), \\ H_3^2 &= H_Z(m_2, m_3, m_4, m_1), H_1^2 = H_Z(m_5, m_1, m_3, m_4), \quad (C.10) \end{aligned}$$

and

$$\begin{aligned} H_X(m_1, m_2, m_3, m_4) &= \frac{1}{(4\pi)^2} \frac{1}{2m_1 p ((m_1 + m_2)^2 + p^2)} \arctan \frac{p}{m_3 + m_4}, \\ H_Y(m_1, m_2, m_3, m_4) &= \frac{1}{(4\pi)^2} \frac{1}{2m_1 p ((p^2 + m_1 + m_4)^2 - 4m_1^2 m_4^2)} \\ & \quad \left((p^2 + m_4^2 - m_1^2) \arctan \frac{p}{m_1 + m_2 + m_3} \right. \\ & \quad \left. + m_1 p \ln \frac{p^2 + (m_1 + m_2 + m_3)^2}{(m_2 + m_3 + m_4)^2} \right), \end{aligned}$$

$$H_2(m_1, m_2, m_3, m_4) = \frac{1}{(4\pi)^2} \frac{1}{2m_2 p (m_4^2 - (m_2 + m_3)^2)} \left(\arctan \frac{p}{m_1 + m_2 + m_3} - \arctan \frac{p}{m_1 + m_4} \right). \quad (\text{C.11})$$

Appendix D

Two-loop Results in the $SU(2)$ Higgs Model

The on-shell value of the Higgs boson self-energy and of the transverse vector boson self-energy to two loops is given in unitary and Feynman gauge in $3 - 2\epsilon$ dimensions, neglecting resummation counter-terms. The coefficients in front of the generic basic two-loop integrals are identical in both gauges. In the unitary gauge result, we therefore write only the part containing products of one-loop integrals. With the following formulae and the one-loop results in [28] and in sect. 2.2, the gauge-invariance of the pole of the Higgs and the vector propagator can easily be proved to two loops.

The two-loop self-energy for the Higgs field in Feynman gauge reads,

$$\begin{aligned} \Sigma^{\xi=1}(p^2 = -M^2) = & \left(-\frac{189}{4} m^4 + \frac{81}{4} M^2 m^2 - \frac{33}{16} M^4 + \frac{3}{8} \frac{M^6}{m^2} \right) F(m, m, m, m) \\ & + \left(3m^4 - 3M^2 m^2 - \frac{3}{4} M^4 + \frac{3}{4} \frac{M^6}{m^2} + \frac{3}{32} \frac{M^8}{m^4} \right) F(m, m, m, m, M) \\ & + \left(9M^2 m^2 - \frac{27}{4} M^4 + \frac{9}{16} \frac{M^8}{m^4} \right) F(m, M, m, M, m) \\ & + \frac{81}{32} \frac{M^8}{m^4} F(M, M, M, M, M) \\ & + \left(\frac{189}{8} m^2 + 6M^2 - \frac{213}{64} \frac{M^4}{m^2} \right) V(m, m, m, m) \\ & + \left(-3m^2 + \frac{3}{2} M^2 + 3 \frac{M^4}{m^2} - \frac{3}{2} \frac{M^6}{m^4} + \frac{15}{64} \frac{M^8}{m^6} \right) V(m, m, m, M) \end{aligned}$$

$$\begin{aligned}
& + \left(-\frac{9}{8}M^2 + \frac{45}{16}\frac{M^4}{m^2} - \frac{9}{64}\frac{M^6}{m^4} \right) V(M, m, M, m) \\
& - \frac{27}{64}\frac{M^6}{m^4} V(M, M, M, M) \\
& + \left(-\frac{567}{2}m^8 + \frac{2097}{4}M^2m^6 - \frac{5061}{16}M^4m^4 + \frac{651}{8}M^6m^2 - \frac{93}{16}M^8 \right) \frac{I_{211}(m, m, m)}{M^2m^2(M^2 - 4m^2)} \\
& + \left(24m^{10} - 18M^2m^8 - \frac{57}{4}M^6m^4 + \frac{81}{8}M^8m^2 - \frac{15}{8}M^{10} \right) \frac{I_{211}(M, m, m)}{M^2m^4(M^2 - 4m^2)} \\
& + \left(-\frac{189}{4}m^6 + \frac{459}{8}M^2m^4 - \frac{111}{4}M^4m^2 + \frac{309}{64}M^6 \right) \\
& + \frac{675}{2}m^6\epsilon - \frac{1449}{4}M^2m^4\epsilon + \frac{2727}{16}M^4m^2\epsilon - \frac{1953}{64}M^6\epsilon \left) \frac{I_{111}(p^2 = -M^2)(m, m, m)}{M^2m^2(M^2 - 4m^2)} \\
& + \left(6m^{10} - \frac{15}{2}M^2m^8 + \frac{27}{8}M^4m^6 - \frac{27}{8}M^6m^4 + \frac{105}{64}M^8m^2 \right. \\
& \left. - \frac{15}{64}M^{10} - 42m^{10}\epsilon + \frac{45}{2}M^2m^8\epsilon - \frac{87}{8}M^4m^6\epsilon + \frac{45}{4}M^6m^4\epsilon \right. \\
& \left. - \frac{171}{32}M^8m^2\epsilon + \frac{51}{64}M^{10}\epsilon \right) \frac{I_{111}(p^2 = -M^2)(M, m, m)}{M^2m^6(M^2 - 4m^2)} \\
& + \left(-\frac{21}{64}\frac{M^4}{m^4} + \frac{81}{32}\frac{M^4}{m^4} \right) \epsilon I_{111}(p^2 = -M^2)(M, M, M) \\
& + \left(\frac{189}{4}m^6 - \frac{711}{8}M^2m^4 + \frac{261}{8}M^4m^2 - \frac{261}{64}M^6 \right. \\
& \left. - \frac{297}{2}m^6\epsilon + \frac{909}{4}M^2m^4\epsilon - \frac{837}{16}M^4m^2\epsilon + \frac{225}{64}M^6\epsilon \right) \frac{I_{111}(0)(m, m, m)}{M^2m^2(M^2 - 4m^2)} \\
& + \left(-6m^{10} + \frac{27}{2}M^2m^8 - \frac{87}{8}M^4m^6 + \frac{45}{8}M^6m^4 - \frac{117}{64}M^8m^2 \right. \\
& \left. + \frac{15}{64}M^{10} + 18m^{10}\epsilon - \frac{63}{2}M^2m^8\epsilon + \frac{111}{8}M^4m^6\epsilon - \frac{9}{8}M^6m^4\epsilon \right. \\
& \left. - \frac{27}{32}M^8m^2\epsilon + \frac{9}{64}M^{10}\epsilon \right) \frac{I_{111}(0)(M, m, m)}{M^2m^6(M^2 - 4m^2)} \\
& + \left(\frac{9}{64}\frac{M^4}{m^4} - \frac{9}{32}\frac{M^4}{m^4} \right) \epsilon I_{111}(0)(M, M, M) \\
& + \left(-\frac{3}{2}m^2 - \frac{9}{16}M^2 - \frac{9}{16}\frac{M^4}{m^2} - \frac{15}{64}\frac{M^6}{m^4} \right) B(p^2 = -M^2)(m^2, m^2)B(p^2 = -M^2)(m^2, m^2) \\
& + \left(-\frac{9}{4}M^2 + \frac{9}{16}\frac{M^4}{m^2} - \frac{9}{32}\frac{M^6}{m^4} \right) B(p^2 = -M^2)(m^2, m^2)B(p^2 = -M^2)(M^2, M^2)
\end{aligned}$$

$$\begin{aligned}
& - \frac{27}{64}\frac{M^6}{m^4} B(p^2 = -M^2)(M^2, M^2)B(p^2 = -M^2)(M^2, M^2) \\
& + \left(36m^{10} + 60M^2m^8 - \frac{99}{2}M^4m^6 + \frac{75}{4}M^6m^4 \right. \\
& \left. - \frac{57}{32}M^8m^2 - \frac{15}{64}M^{10} \right) \frac{B(p^2 = -M^2)(m^2, m^2)A(m^2)}{M^2m^6(M^2 - 4m^2)} \\
& + \left(-6m^{10} + 18M^2m^8 - \frac{39}{4}M^4m^6 + \frac{45}{8}M^6m^4 \right. \\
& \left. - \frac{63}{32}M^8m^2 + \frac{15}{64}M^{10} \right) \frac{B(p^2 = -M^2)(m^2, m^2)A(M^2)}{M^2m^6(M^2 - 4m^2)} \\
& + \left(\frac{27}{4}M^2m^4 + \frac{27}{8}M^4m^2 - \frac{27}{16}M^6 \right) \frac{B(p^2 = -M^2)(M^2, M^2)A(m^2)}{m^4(M^2 - 4m^2)} \\
& + \left(27m^8 - \frac{39}{4}M^2m^6 + \frac{33}{32}M^6m^2 - \frac{15}{64}M^8 \right) \frac{A(m^2)A(M^2)}{M^2m^6(M^2 - 4m^2)} \\
& + \left(\frac{57}{4}m^6 - \frac{51}{32}M^4m^2 + \frac{15}{64}M^6 \right) \frac{A(m^2)A(M^2)}{m^6(M^2 - 4m^2)} \\
& - \frac{9}{16}\frac{M^2}{m^4} A(M^2)A(M^2). \tag{D.1}
\end{aligned}$$

The vector boson self-energy in Feynman gauge is to two-loop order,

$$\begin{aligned}
\Pi_T^{\xi=1}(p^2 = -m^2) &= \frac{849}{32}m^4 F(m, m, m, m) \\
& + \left(-\frac{63}{8}m^4 + \frac{27}{8}M^2m^2 - \frac{11}{32}M^4 + \frac{1}{16}\frac{M^6}{m^2} \right) F(m, m, m, M) \\
& + \left(-\frac{63}{2}m^4 + \frac{27}{2}M^2m^2 - \frac{11}{8}M^4 + \frac{1}{4}\frac{M^6}{m^2} \right) F(M, m, m, m) \\
& + \left(m^4 - M^2m^2 - \frac{1}{4}M^4 + \frac{1}{4}\frac{M^6}{m^2} + \frac{1}{32}\frac{M^8}{m^4} \right) F(M, m, m, M) \\
& + \left(\frac{3}{2}M^2m^2 - \frac{9}{8}M^4 + \frac{3}{32}\frac{M^8}{m^4} \right) F(m, m, M, M) \\
& + \left(-\frac{2115}{64}m^2 + M^2 - \frac{1}{4}\frac{M^4}{m^2} \right) V(m, m, m, m) \\
& + \left(\frac{63}{8}m^2 + 2M^2 - \frac{71}{64}\frac{M^4}{m^2} \right) V(m, M, m, m) \\
& + \left(\frac{3}{2}\frac{m^4}{M^2} + \frac{1}{2}m^2 - \frac{9}{8}M^2 - \frac{3}{16}\frac{M^4}{m^2} - \frac{17}{128}\frac{M^6}{m^4} \right) V(m, m, M, m)
\end{aligned}$$

$$\begin{aligned}
& + \left(\frac{63}{16} m^2 + M^2 - \frac{71}{128} \frac{M^4}{m^2} \right) V(M, m, m, m) \\
& + \left(-\frac{1}{2} m^2 + \frac{1}{4} M^2 + \frac{1}{2} \frac{M^4}{m^2} - \frac{1}{4} \frac{M^6}{m^4} + \frac{5}{128} \frac{M^8}{m^6} \right) V(M, M, m, m) \\
& + \left(\frac{3}{8} M^2 + \frac{3}{4} \frac{M^4}{m^2} - \frac{15}{64} \frac{M^6}{m^4} \right) V(m, M, M, M) \\
& + \left(\frac{189}{4} m^8 - \frac{699}{8} M^2 m^6 + \frac{1687}{32} M^4 m^4 - \frac{217}{16} M^6 m^2 + \frac{31}{32} M^8 \right) \frac{I_{211}(m, m, M)}{m^4(M^2 - 4m^2)} \\
& + \left(-4m^{10} + \frac{9}{2} M^4 m^6 + \frac{1}{2} M^6 m^4 - \frac{21}{16} M^8 m^2 + \frac{5}{16} M^{10} \right) \frac{I_{211}(M, m, M)}{m^6(M^2 - 4m^2)} \\
& + \left(\frac{3}{2} m^8 + \frac{1021}{16} M^2 m^6 - \frac{997}{64} M^4 m^4 - \frac{1}{2} M^6 m^2 + \frac{13}{128} M^8 \right. \\
& \left. - \frac{21}{2} m^8 \epsilon - \frac{1881}{4} M^2 m^6 \epsilon + \frac{1851}{16} M^4 m^4 \epsilon + \frac{5}{8} M^6 m^2 \epsilon - \frac{5}{128} M^8 \epsilon \right) \frac{I_{111}(p^2 = -m^2)(m, m, m)}{M^2 m^4 (M^2 - 4m^2)} \\
& + \left(-15m^6 + \frac{799}{64} M^2 m^4 - \frac{559}{128} M^4 m^2 + \frac{31}{64} M^6 \right. \\
& \left. + \frac{1617}{16} m^6 \epsilon - \frac{2251}{32} M^2 m^4 \epsilon + \frac{737}{32} M^4 m^2 \epsilon - \frac{41}{16} M^6 \epsilon \right) \frac{I_{111}(p^2 = -m^2)(M, m, m)}{m^4(M^2 - 4m^2)} \\
& + \left(-\frac{1}{2} m^8 + \frac{9}{8} M^2 m^6 - \frac{13}{16} M^4 m^4 + \frac{1}{16} M^6 m^2 + \frac{5}{128} M^8 \right. \\
& \left. - 2m^8 \epsilon - \frac{23}{4} M^2 m^6 \epsilon + \frac{9}{8} M^4 m^4 \epsilon + \frac{1}{64} M^6 m^2 \epsilon - \frac{3}{32} M^8 \epsilon \right) \frac{I_{111}(p^2 = -m^2)(M, M, m)}{m^6(M^2 - 4m^2)} \\
& + \left(-\frac{63}{2} m^6 - \frac{951}{16} M^2 m^4 + \frac{483}{32} M^4 m^2 + \frac{87}{128} M^6 \right. \\
& \left. 99m^6 \epsilon + \frac{1647}{16} M^2 m^4 \epsilon - \frac{1101}{32} M^4 m^2 \epsilon + \frac{3}{32} M^6 \epsilon \right) \frac{I_{111}(0)(m, m, m)}{M^2 m^2 (M^2 - 4m^2)} \\
& + \left(\frac{9}{2} m^6 + \frac{17}{2} M^2 m^4 - 9M^4 m^2 + \frac{7}{2} M^6 - \frac{41}{128} \frac{M^8}{m^2} - \frac{5}{128} \frac{M^{10}}{m^4} \right. \\
& \left. - \frac{27}{2} m^6 \epsilon - \frac{29}{2} M^2 m^4 \epsilon + \frac{49}{4} M^4 m^2 \epsilon - \frac{21}{4} M^6 \epsilon + \frac{149}{128} \frac{M^8}{m^2} \epsilon - \frac{1}{16} \frac{M^{10}}{m^4} \epsilon \right) \frac{I_{111}(0)(M, m, m)}{M^2 m^2 (M^2 - 4m^2)} \\
& + \left(\frac{9}{8} M^2 m^4 + \frac{3}{4} M^4 m^2 - \frac{21}{64} M^6 - \frac{3}{4} M^2 m^4 \epsilon + \frac{3}{16} M^4 m^2 \epsilon + \frac{9}{64} M^6 \epsilon \right) \frac{I_{111}(0)(M, M, M)}{m^4(M^2 - 4m^2)} \\
& + \left(\frac{45}{16} m^2 + \frac{1}{4} M^2 - \frac{1}{16} \frac{M^4}{m^2} \right) B(p^2 = -m^2)(m^2, m^2) B(p^2 = -m^2)(m^2, m^2) \\
& + \left(\frac{9}{2} m^2 - \frac{5}{4} M^2 + \frac{1}{2} \frac{M^4}{m^2} \right) B(p^2 = -m^2)(m^2, m^2) B(p^2 = -m^2)(M^2, m^2)
\end{aligned}$$

$$\begin{aligned}
& + \left(-\frac{1}{2} m^2 + \frac{5}{8} M^2 - \frac{1}{8} \frac{M^4}{m^2} \right) B(p^2 = -m^2)(M^2, m^2) B(p^2 = -m^2)(M^2, m^2) \\
& + \left(-54m^6 - \frac{963}{8} M^2 m^4 + \frac{63}{2} M^4 m^2 + \frac{63}{64} M^6 \right) \frac{B(p^2 = -m^2)(m^2, m^2) A(m^2)}{M^2 m^2 (M^2 - 4m^2)} \\
& + \left(\frac{63}{4} m^6 - \frac{207}{8} M^2 m^4 + \frac{135}{16} M^4 m^2 - \frac{63}{64} M^6 \right) \frac{B(p^2 = -m^2)(m^2, m^2) A(M^2)}{M^2 m^2 (M^2 - 4m^2)} \\
& + \left(9m^{10} + \frac{9}{2} M^2 m^8 - \frac{35}{4} M^4 m^6 + \frac{9}{2} M^6 m^4 \right. \\
& \left. - \frac{35}{64} M^8 m^2 - \frac{5}{128} M^{10} \right) \frac{B(p^2 = -m^2)(M^2, m^2) A(m^2)}{M^2 m^6 (M^2 - 4m^2)} \\
& + \left(-m^{10} + M^2 m^8 - \frac{9}{8} M^4 m^6 + \frac{7}{8} M^6 m^4 \right. \\
& \left. - \frac{5}{16} M^8 m^2 + \frac{5}{128} M^{10} \right) \frac{B(p^2 = -m^2)(M^2, m^2) A(M^2)}{M^2 m^6 (M^2 - 4m^2)} \\
& + \left(18m^{10} - 39M^2 m^8 + \frac{51}{4} M^4 m^6 + \frac{11}{32} M^6 m^4 \right. \\
& \left. - \frac{11}{32} M^8 m^2 + \frac{5}{128} M^{10} \right) \frac{A(m^2) A(M^2)}{M^4 m^6 (M^2 - 4m^2)} \\
& + \left(3m^{10} + M^2 m^8 - \frac{19}{8} M^4 m^6 - \frac{17}{16} M^6 m^4 \right. \\
& \left. + \frac{29}{64} M^8 m^2 - \frac{5}{128} M^{10} \right) \frac{A(m^2) A(M^2)}{M^4 m^6 (M^2 - 4m^2)} \\
& + \left(\frac{1}{2} m^6 + \frac{1}{8} M^2 m^4 + \frac{11}{32} M^4 m^2 - \frac{7}{64} M^6 \right) \frac{A(M^2) A(M^2)}{M^2 m^4 (M^2 - 4m^2)}. \tag{D.2}
\end{aligned}$$

In unitary gauge, the products of one-loop integrals in the two-loop self-energies of the Higgs field read,

$$\begin{aligned}
& \Sigma^{\xi=\infty}(p^2 = -M^2) = \dots \\
& + \left(-\frac{3}{2} m^2 + \frac{27}{16} M^2 - \frac{27}{16} \frac{M^4}{m^2} + \frac{3}{64} \frac{M^6}{m^4} \right) B(p^2 = -M^2)(m^2, m^2) B(p^2 = -M^2)(m^2, m^2) \\
& + \left(-\frac{9}{4} M^2 + \frac{9}{16} \frac{M^4}{m^2} + \frac{9}{16} \frac{M^6}{m^4} \right) B(p^2 = -M^2)(m^2, m^2) B(p^2 = -M^2)(M^2, M^2) \\
& - \frac{27}{64} \frac{M^6}{m^4} B(p^2 = -M^2)(M^2, M^2) B(p^2 = -M^2)(M^2, M^2)
\end{aligned}$$

$$\begin{aligned}
& + \left(36m^{10} + 51M^2m^8 - \frac{207}{4}M^4m^6 + \frac{33}{2}M^6m^4 \right. \\
& - \left. \frac{15}{16}M^8m^2 - \frac{15}{64}M^{10} \right) \frac{B(p^2 = -M^2)(m^2, m^2)A(m^2)}{M^2m^6(M^2 - 4m^2)} \\
& + \left(-6m^{10} + 18M^2m^8 - \frac{39}{4}M^4m^6 + \frac{27}{8}M^6m^4 \right. \\
& - \left. \frac{45}{32}M^8m^2 + \frac{15}{64}M^{10} \right) \frac{B(p^2 = -M^2)(m^2, m^2)A(M^2)}{M^2m^6(M^2 - 4m^2)} \\
& + \left(\frac{27}{4}M^2m^4 - \frac{27}{32}M^6 \right) \frac{B(p^2 = -M^2)(M^2, M^2)A(m^2)}{m^4(M^2 - 4m^2)} \\
& + \left(27m^8 - \frac{75}{4}M^2m^6 + \frac{51}{32}M^6m^2 - \frac{15}{64}M^8 \right) \frac{A(m^2)A(M^2)}{M^2m^6(M^2 - 4m^2)} \\
& + \left(\frac{57}{4}m^6 - \frac{9}{4}M^2m^4 - \frac{33}{32}M^4m^2 + \frac{15}{64}M^6 \right) \frac{A(m^2)A(M^2)}{m^6(M^2 - 4m^2)} \\
& - \frac{9}{16} \frac{M^2}{m^4} A(M^2)A(M^2), \tag{D.3}
\end{aligned}$$

and for the vector field,

$$\begin{aligned}
& \Pi_T^{\xi=\infty}(p^2 = -m^2) = \dots \\
& + \left(-\frac{99}{32}m^2 + \frac{1}{4}M^2 - \frac{1}{16} \frac{M^4}{m^2} \right) B(p^2 = -m^2)(m^2, m^2)B(p^2 = -m^2)(m^2, m^2) \\
& + \left(\frac{21}{4}m^2 - \frac{13}{8}M^2 + \frac{19}{32} \frac{M^4}{m^2} \right) B(p^2 = -m^2)(m^2, m^2)B(p^2 = -m^2)(M^2, m^2) \\
& + \left(-\frac{1}{2}m^2 + \frac{5}{8}M^2 - \frac{1}{8} \frac{M^4}{m^2} \right) B(p^2 = -m^2)(M^2, m^2)B(p^2 = -m^2)(M^2, m^2) \\
& + \left(-63m^6 - \frac{555}{8}M^2m^4 + \frac{315}{16}M^4m^2 + \frac{57}{64}M^6 \right) \frac{B(p^2 = -m^2)(m^2, m^2)A(m^2)}{M^2m^2(M^2 - 4m^2)} \\
& + \left(\frac{63}{4}m^6 - \frac{219}{8}M^2m^4 + \frac{135}{16}M^4m^2 - \frac{57}{64}M^6 \right) \frac{B(p^2 = -m^2)(m^2, m^2)A(M^2)}{M^2m^2(M^2 - 4m^2)} \\
& + \left(9m^{10} - \frac{3}{2}M^2m^8 - \frac{17}{4}M^4m^6 + 3M^6m^4 \right. \\
& - \left. \frac{23}{64}M^8m^2 - \frac{5}{128}M^{10} \right) \frac{B(p^2 = -m^2)(M^2, m^2)A(m^2)}{M^2m^6(M^2 - 4m^2)} \\
& + \left(-m^{10} + M^2m^8 - \frac{9}{8}M^4m^6 + \frac{7}{8}M^6m^4 \right.
\end{aligned}$$

$$\begin{aligned}
& - \frac{5}{16}M^8m^2 + \frac{5}{128}M^{10} \left) \frac{B(p^2 = -m^2)(M^2, m^2)A(M^2)}{M^2m^6(M^2 - 4m^2)} \\
& + \left(18m^{10} - 57M^2m^8 + \frac{81}{4}M^4m^6 + \frac{11}{32}M^6m^4 \right. \\
& - \left. \frac{17}{32}M^8m^2 + \frac{5}{128}M^{10} \right) \frac{A(m^2)A(M^2)}{M^4m^6(M^2 - 4m^2)} \\
& + \left(3m^{10} + M^2m^8 - \frac{43}{8}M^4m^6 - \frac{17}{16}M^6m^4 \right. \\
& + \left. \frac{41}{64}M^8m^2 - \frac{5}{128}M^{10} \right) \frac{A(m^2)A(M^2)}{M^4m^6(M^2 - 4m^2)} \\
& + \left(\frac{1}{2}m^6 + \frac{1}{8}M^2m^4 + \frac{11}{32}M^4m^2 - \frac{7}{64}M^6 \right) \frac{A(M^2)A(M^2)}{M^2m^4(M^2 - 4m^2)}. \tag{D.4}
\end{aligned}$$

Appendix E

Numerical Evaluation of the Master Integral

All basic integrals except for the master integral $F(m_1, m_2, m_3, m_4, m_5)$ have analytic results. It can be represented by a one-dimensional integral as shown in appendix C. If all masses are equal and with $p^2 = m^2$, it reads,

$$F(m, m, m, m, m) = -\frac{\sqrt{2}}{32\pi^2 m^4} \int_0^1 \frac{dx}{(x+2)\sqrt{3-x^2}} (\ln 3 + (x+1)\ln(x+3) - (2x+4)\ln(x+2) + (x+3)\ln(x+1)). \quad (\text{E.1})$$

In the following table, we investigate the master integral for two different masses in its argument. We give the numerical results for the cases of interest in the analysis of chapter 5.

$z = \frac{M}{m}$	1	1.2	1.4	1.6	1.8
$F(m, m, m, m, m) \cdot 10^4 m^4$	2.4531	2.4531	2.4531	2.4531	2.4531
$F(m, m, m, m, M) \cdot 10^4 m^4$	2.4531	2.1332	1.8723	1.6567	1.4763
$F(M, m, m, m, m) \cdot 10^4 m^4$	2.4531	2.0291	1.7113	1.4659	1.2716
$F(M, m, m, M, m) \cdot 10^4 m^4$	2.4531	1.6834	1.2062	0.89441	0.68080
$F(m, m, M, M, M) \cdot 10^4 m^4$	2.4531	1.4776	0.95061	0.64266	0.45158

Table 2: Numerical results for the master integral

Bibliography

- [1] E. W. Kolb and M. S. Turner, *The Early Universe*, (Addison-Wesley Publishing Company, 1990)
- [2] A. D. Sakharov, JETP Letters 5 (1967) 24
- [3] For a review and references, see V. A. Rubakov and M. E. Shaposhnikov, Phys. Usp. **39** (1996) 461
- [4] D. A. Kirzhnits and A. D. Linde, Phys. Lett. B **72** (1972) 471
- [5] For a discussion and references, see K. Jansen, Nucl. Phys. B (Proc. Supp.) **47** (1996) 196
- [6] For a recent review, see R. H. Brandenberger, *Particle Physics Aspects of Modern Cosmology*, to be published in *Field Theoretical Methods in Fundamental Physics*, ed. by Choonkyu Lee, Mineumsa Co. Ltd., Seoul, 1997, Preprint BROWN-HET-1067, hep-ph/9701276
- [7] For a discussion and references, see M. Plümacher, DESY-THESIS-1998-009
- [8] For a discussion and references, see Proceedings of *Strong and Electroweak Matter 1997*, (World Scientific, 1998)
- [9] A. D. Linde, Phys. Lett. B **96** (1980) 289;
D. Gross, R. Pisarski and L. Yaffe, Rev. Mod. Phys. **53** (1981) 43
- [10] A. Jakovác, K. Kajantie and A. Patkós, Phys. Rev. D **49** (1994) 6810;
K. Farakos, K. Kajantie, K. Rummukainen and M. Shaposhnikov, Nucl. Phys. B **425** (1994) 67
- [11] For a discussion and references, see J. I. Kapusta, *Finite Temperature Field Theory*, (Cambridge University Press, 1989)
- [12] E. Braaten and R. Pisarski, Nucl. Phys. B **337** (1990) 569
- [13] D. Gross, R. Pisarski and L. Yaffe, Rev. Mod. Phys. **53** (1981) 43
- [14] P. Arnold and O. Espinosa, Phys. Rev. D **47** (1993) 3546
- [15] L. Dolan and R. Jackiw, Phys. Rev. D **9** (1974) 3320
- [16] W. Buchmüller, Z. Fodor, T. Helbig and D. Walliser, Ann. Phys. **234** (1994) 260
- [17] K. Farakos, K. Kajantie, K. Rummukainen and M. Shaposhnikov, Nucl. Phys. B **442** (1995) 317
- [18] T. Appelquist and R. Pisarski, Phys. Rev. D **23** (1981) 2305
S. Nadkarni, Phys. Rev. D **27** (1983) 917
N. P. Landsman, Nucl. Phys. B **322** (1989) 498
P. Lacock, D. E. Miller and T. Reisz, Nucl. Phys. B **369** (1992) 501
L. Kärkkäinen, P. Lacock, B. Petersson and T. Reisz, Nucl. Phys. B **395** (1993) 733
- [19] M. Carrington, Phys. Rev. D **45** (1992) 2933
- [20] O. Philipsen, M. Teper and H. Wittig, Nucl. Phys. B **469** (1996) 445
- [21] F. Karsch, T. Neuhaus, A. Patkós and J. Rank, Nucl. Phys. B **474** (1996) 217
- [22] W. Buchmüller and O. Philipsen, Phys. Lett. B **397** (1997) 112
- [23] B. Grossmann, S. Gupta, U. M. Heller and F. Karsch, Nucl. Phys. B **417** (1994) 289
H.-G. Dosch, J. Kripfganz, A. Laser and M. G. Schmidt, Phys. Lett. B **365** (1995) 213
- [24] M. Laine and O. Philipsen, hep-lat/9711022
- [25] M. Teper, Phys. Lett. B **289** (1992) 115
- [26] A. K. Rebhan, Phys. Rev. D **48** (1993) 3967
- [27] I. Montvay and G. Münster, *Quantum Fields on a Lattice*, (Cambridge University Press, 1994)
- [28] W. Buchmüller and O. Philipsen, Nucl. Phys. B **443** (1995) 47
- [29] L. Dolan and R. Jackiw, Phys. Rev. D **9** (1974) 2904
- [30] O. Philipsen, Doctoral Thesis

- [31] L. H. Ryder, *Quantum Field Theory*, (Cambridge University Press, 1985)
- [32] B. W. Lee and J. Zinn-Justin, Phys. Rev. D **5** (1972) 3121, 3137, 3155, D **7** (1973) 1049
K. Fujikawa, B. W. Lee and A. I. Sanda, Phys. Rev. D **6** (1972) 2923
E. S. Abers and B. W. Lee, Phys. Rep. **9** (1973) 1
S. Weinberg, Phys. Rev. D **7** (1973) 2887
T. D. Lee and C. N. Yang, Phys. Rev. **128** (1962) 885
- [33] I. Gerstein, R. Jackiw, B. Lee and S. Weinberg, Phys. Rev. D **3** (1971) 2486
- [34] G. Alexanian and V. P. Nair, Phys. Lett. B **352** (1995) 435
- [35] R. Jackiw and S.-Y. Pi, Phys. Lett. B **368** (1996) 131
- [36] J. M. Cornwall, Phys. Rev. D **57** (1998) 3694
- [37] O. V. Tarasov, Nucl. Phys. B **502** (1997) 455, and refernces therein
- [38] G. Weiglein, R. Scharf and M. Böhm, Nucl. Phys. B **416** (1994) 606
G. Weiglein, R. Mertig, R. Scharf and M. Böhm, *New computing techniques in physics research II*, ed. D. Perret-Gallix (World Scientific, Singapore, 1992)
- [39] J. A. M. Vermaseren, *Symbolic manipulation with FORM*. Amsterdam, Computer Algebra Nederland, 1991
- [40] A. K. Rajantie, Nucl. Phys. B **480** (1996) 729
- [41] R. Jackiw and S.-Y. Pi, Phys. Lett. B **403** (1997) 297
- [42] I. Gerstein, R. Jackiw, B. Lee and S. Weinberg, Phys. Rev. D **3** (1971) 2486
- [43] A. K. Rajantie, Nucl. Phys. B **513** (1998) 761
- [44] M. Teper, Phys. Lett. B **311** (1993) 223
D. Karabali, C. Kim and V. P. Nair, hep-th/9804132
- [45] O. Philipsen, M. Teper and H. Wittig, Nucl. Phys. B **469** (1996) 445
- [46] F. Eberlein, DESY-98-048, hep-ph/9804460

Acknowledgments

I am most grateful to my advisor, Prof. W. Buchmüller, for continuous encouragement and highly instructive discussions and comments.

I would like to thank O. Tarasov for valuable support when implementing the reduction method and for an independent calculation of eq. (4.13).

I would also like to acknowledge fruitful discussions with O. Philipsen, A. Jakovác, Y. Schröder and T. Plehn.

Finally, I would like to thank all my friends, and in particular Moritz and Dodo for their encouragement and patience.

